A Comprehensive Review of Remaining Useful Life Estimation Approaches for Rotating Machinery

Shahil Kumar [1], Krish Kumar Raj [1], Maurizio Cirrincione [1], Giansalvo Cirrincione [2], Vincenzo Franzitta [3,*] and Rahul Ranjeev Kumar [1]

[1] School of Information Technology, Engineering, Mathematics and Physics, The University of the South Pacific, Private Mail Bag Laucala Campus, Suva 1168, Fiji; s11171249@student.usp.ac.fj (S.K.); krish.raj@usp.ac.fj (K.K.R.); maurizio.cirrincione@usp.ac.fj (M.C.); rahul.kumar@usp.ac.fj (R.R.K.)

[2] Laboratory of Novel Technologies, University of Picardie Jules Verne, 80000 Amiens, France; giansalvo.cirrincione@u-picardie.fr

[3] Department of Engineering, University of Palermo, 90128 Palermo, Italy

* Correspondence: vincenzo.franzitta@unipa.it

Abstract: This review paper comprehensively analyzes the prognosis of rotating machines (RMs), focusing on mechanical-flaw and remaining-useful-life (RUL) estimation in industrial and renewable energy applications. It introduces common mechanical faults in rotating machinery, their causes, and their potential impacts on RM performance and longevity, particularly in wind, wave, and tidal energy systems, where reliability is crucial. The study outlines the primary procedures for RUL estimation, including data acquisition, health indicator (HI) construction, failure threshold (FT) determination, RUL estimation approaches, and evaluation metrics, through a detailed review of published work from the past six years. A detailed investigation of HI design using mechanical-signal-based, model-based, and artificial intelligence (AI)-based techniques is presented, emphasizing their relevance to condition monitoring and fault detection in offshore and hybrid renewable energy systems. The paper thoroughly explores the use of physics-based, data-driven, and hybrid models for prognosis. Additionally, the review delves into the application of advanced methods such as transfer learning and physics-informed neural networks for RUL estimation. The advantages and disadvantages of each method are discussed in detail, providing a foundation for optimizing condition-monitoring strategies. Finally, the paper identifies open challenges in prognostics of RMs and concludes with critical suggestions for future research to enhance the reliability of these technologies.

Keywords: bearings; condition monitoring; fault diagnosis; gearbox; health indicators; misalignment; prognosis; rotating machines; remaining useful life

1. Introduction

Fault diagnosis and prognosis of RMs are crucial in industrial equipment maintenance, aiding in preventing unexpected machinery failures and unplanned downtime [1,2]. Turbines, compressors, pumps, fans, motors, and generators are just a few of the many parts that make up RMs. These parts are essential to a number of industries, including manufacturing, transportation, oil and gas, and power generation. For instance, compressors and pumps are essential for fluid and gas transfer systems, while turbines—such as gas, steam, and wind turbines—are frequently employed for energy conversion. For precise maintenance planning, distinct RUL estimation approaches are required for each of these components, due to their unique degradation and failure mechanisms. Pumps and compressors may encounter cavitation or corrosion, whereas turbines, for example, are subject to high amounts of stress from varying loads, which may result in blade or rotor fatigue. Early diagnosis of insulation failure, misalignment, or rotor imbalance can greatly extend the operating life of motors and generators, which are essential for powering a variety of industrial operations and renewable energy systems [3].

RMs, including motors, generators, and pumps are crucial to performance in the renewable energy sector, especially in offshore wind farms and hybrid renewable systems, where dependable operation is necessary for maximum efficiency. These machines' dependability can be significantly diminished by misalignment, gearbox issues, and bearing issues, which can lead to expensive downtime and decreased energy output [4]. This is particularly crucial in offshore settings, where equipment access is more difficult and maintenance expenses are higher.

Even though larger parts like turbines, motors, and generators are essential to the functioning of industrial systems, the most serious and expensive malfunctions are frequently caused by small flaws in parts like bearings, gears, and misalignment. For instance, poor lubrication or contamination can cause bearing problems to develop gradually, which might ultimately result in excessive vibrations and unequal load distribution. If these minor issues are not fixed right away, they may spread and compromise larger parts like shafts or gears, leading to more significant failures that impact the entire system. Even small misalignments may place greater stress on gears and bearings, accelerating wear and perhaps resulting in catastrophic failures if ignored.

Thus, while bearing, gear, and misalignment defects can appear to be minor in comparison to major component failures, they frequently serve as early warning signs of more serious problems. Companies can avoid significant system failures and cut down on expensive downtime by accurately forecasting the RUL of these smaller components. Therefore, proactive maintenance that relies on the early estimation of the RUL of these minor issues is essential for guaranteeing the dependability and effectiveness of massive, intricate machinery.

Data-driven methods have become the predominant approach for remaining-useful-life (RUL) estimation, relying on historical data and statistical models to deliver accurate predictions [5]. These methods are adept at learning complex patterns from large datasets, which enables them to provide reliable prognoses under varying operating conditions. By estimating the remaining operational time before a component's failure, RUL predictions support the implementation of preventive maintenance plans, thus potentially extending the component's lifespan. Deep learning (DL)-based techniques, in particular, can enhance the reliability and efficiency of industrial machinery through precise RUL estimations [1]. Prognosis using DL can effectively predict future component health in RMs, allowing for timely maintenance and reducing the risk of sudden failures. DL methods, including convolutional neural networks (CNNs), recurrent neural networks (RNNs), and temporal fusion transformers, are particularly effective for these tasks, due to their ability to handle large, unstructured datasets and adapt to diverse fault types. For instance, CNNs can process high-dimensional vibration data to identify subtle anomalies, while RNNs and long short-term memory (LSTM)-based models are well-suited for capturing temporal dependencies in time-series data, which is critical for accurate RUL predictions. Transformers, with their attention mechanisms, excel in isolating important features within extended time-series sequences, enabling more precise diagnostics and prognostics, even under fluctuating conditions. In this context, prognostics and health management (PHM) has emerged as a vital field that systematically monitors the health of engineering systems and their key components. PHM integrates essential functions, including establishing HIs, predicting RUL, and developing health management strategies. HIs, in particular, are essential for assessing the current status of components and tracking long-term health trends [6].

RUL estimation plays a pivotal role in predictive maintenance strategies, enabling organizations to proactively manage and schedule maintenance activities, thereby reducing downtime and extending the operational lifespan of critical machinery and equipment. A rapidly increasing trend has been seen in the number of these publications [7]. In addition, several review papers have been published in the past years outlining the attributes of RUL estimation. For instance, Heng et al. [8] published a study based on the merits and weaknesses of RUL prediction techniques up to 2009. An industrial application

approach was used by Sikorska et al. [9] to perform a similar analysis on RUL estimation approaches till 2009. Kan et al. [10] reviewed the prognostic techniques for non-stationary and non-linear rotating systems. Si et al. [11] presented statistical data-driven approaches and provided a comprehensive review of the primary methodologies for RUL prediction. Lee et al. [12] conducted a review on the development of PHM systems up to 2010, offering a guide to assist in choosing an RUL estimation method by comparing their advantages and disadvantages. Wang et al. [6] conducted an extensive review on vibration-based HIs for bearings and gears, covering the construction of these indicators through mechanical signal processing, modeling, and machine learning techniques till 2017. Lei et al. [7] provided a review of the whole process of RUL estimation till 2017. The authors in [13] reviewed degradation data analysis and RUL estimation; however, their study was limited to only Wiener-process-based methods. Moreover, Zio et al. [14] focused on identifying the primary challenges and future directions for the comprehensive implementation of condition-based and predictive maintenance in real-world applications.

While the publications mentioned above have provided tremendous insight into the RUL estimation process, it must be noted that they have the following limitations. Most of these papers were published more than five years ago; therefore, a new review must be conducted to cover every step in RUL prediction. The paper in [6] only focused on HI construction for RUL estimation, and Ref. [11] only concentrated on statistical data-driven approaches. The papers also did not cover the whole process of RUL prediction, except for [7].

The authors of this study fill these gaps by providing a review of the five steps of RUL estimation in detail. These include (1) data acquisition, (2) feature engineering for HI construction, (3) failure threshold (FT) selection, (4) RUL estimation techniques, and (5) evaluation metrics. The RUL estimation process is divided into five steps for several key reasons. Firstly, this division provides a structured framework that systematically addresses the essential components involved in RUL estimation, helping to organize the review and guide readers through the process logically. Secondly, it ensures comprehensive coverage, as each step represents a critical aspect of the RUL estimation process, from the initial data collection to final evaluation. Thirdly, this focus on five distinct steps allows for clarity and precision in defining and discussing each stage's specific methodologies, challenges, and advancements. In addition, this study provides a review of the transfer-learning-based approaches and physics-informed neural-network-based approaches used for RUL estimation, which have gained increased attention in the past few years. Figure 1 shows the generic flow of the RUL estimation process, highlighting each major step of RUL estimation.

Regarding the database used, journal articles, books, and conference proceedings of standard engineering repositories were consulted (IEEE Xplore, Elsevier, Springer, MDPI, Wiley, and others, as per the references). Up to 90% of the publications reviewed concerning RUL estimation are journal articles, with the majority of them spanning between 2017 and 2024. In addition, the remaining 10% contained books, technical reports, and conference proceedings spanning the past decade. Some very recent exceptional review papers were also used in conducting this review. The authors took utmost care in searching the databases for literature, such that all relevant information is covered about the fundamentals of the prognosis of RMs.

The major contributions of this study are as follows:

1. This paper provides a review of literature from the past decade related to the prognostics of mechanical components in RMs, with the majority of publications reviewed being from the past six years.
2. This study divides the complete RUL estimation process into five significant steps and reviews them in detail.
3. This study discusses the feature engineering step in detail, which is essential for HI construction.

4. This study provides a list of the publicly available run-to-failure datasets, which are essential for RUL estimation purposes.

The rest of this paper is outlined as follows. Section 2 presents an overview of the common types of mechanical faults that occur in RMs and briefly describes the causes and consequences of each failure. Section 3 discusses PHM, which includes RUL fundamentals and a review of the recent methodologies used in RUL estimation. Finally, Section 4 provides some open challenges and future prospects concerning the prognosis of RMs.
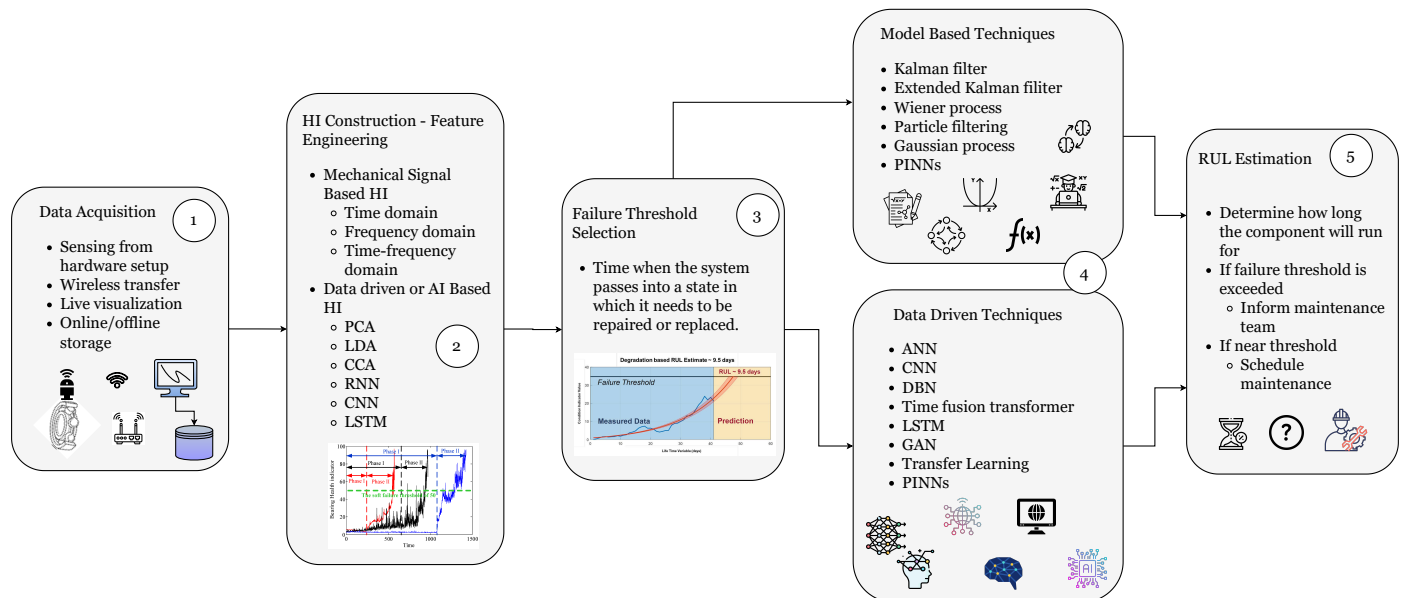
Figure 1. A generic framework for RUL estimation.

2. Mechanical Faults in RMs

RMs are essential in many industrial fields, including manufacturing, transportation, and power generation. Turbines, motors, generators, and other rotating machinery are all necessary to transform mechanical energy into meaningful work. Due to their intricate mechanical and electrical components, these machines provide effectiveness, dependability, and diversity, yet they are liable to various undesirable faults.

The most commonly used are IMs, which are made up of both electrical and mechanical components, which include the rotor, shaft, stator, windings, and bearings. Rolling element bearings and gearboxes are the core components of RMs and are used to support the operation of the machinery [15]. The most common faults in these types of machinery are mechanical faults, which include bearing faults, misalignment faults, and gearbox faults [16]. Table 1 presents a summary of various mechanical faults, their causes, and the resulting consequences. It highlights the different factors that lead to bearing faults, gearbox faults, and misalignment faults and describes the specific impacts each type of fault has on the mechanical components of RMs. In addition, the specific details and the link between the causes and consequences of each fault type are discussed in the following subsections, starting with a detailed analysis of rolling bearing faults, followed by gear faults, and finally, misalignment faults.

Table 1. A summary of mechanical faults, their causes, and the consequences of these faults.

Fault	Causes	Consequences
Bearing fault	• Increase in shaft voltage above the insulating capability of the bearing grease • Shaft misalignment/imbalance • Overload • Loss/contamination of lubricants • Manufacturing flaws • Increased temperatures	• Excessive vibration and eventual bearing failure • Accelerated wear on rotating components • Ripple in output torque • Ripple in current harmonic spectrum at definite frequency • Eccentricity faults
Gearbox fault	• Overload • Improper lubrication • Misalignment • Frosting • Surface contamination • Manufacturing flaws	• Dynamic Instabilities (vibrations) • Fluctuations in load transmitted to the driven machinery • Mechanical losses in the power transmission system • Structural Fatigue
Misalignment fault	• Incorrect alignment of drive shaft with load • Center of mass does not lie on the axis of rotation, i.e., heavy spot on rotor • Installation errors • Failure in bearings	• Premature wear to mechanical drive components • Vibration being fed into both the load and the motor drive shaft • Eccentricity faults • Gear and bearing damage

2.1. Rolling Bearing Faults

Bearing faults make up to 30–50% of all faults in IMs [17–19]. A bearing is the component that supports and allows for the smooth rotation of the rotor shaft [20]. Bearings must be regularly inspected and lubricated to prevent wear and potential failure [21]. A bearing has four components: an inner raceway, an outer raceway, balls, and a cage that provides an equidistant arrangement between the balls. There are four corresponding faults associated with these components: inner race faults, outer race faults, rolling element faults, and cage faults. An additional fault could be a combination of any of the four faults mentioned above. When there is a fault on the surface of an inner or outer race in a bearing, the impacts caused by the rollers striking the imperfection excite resonant frequency bands and induce transients over time [6]. The fault frequencies at which these faults can be detected are provided in Equations (1)–(4) [22]. The structure of a rolling bearing can be seen in Figure 2a, with the faults that can occur in Figure 2b.

$$Inner_{ring\,defect\,frequency} = \frac{N_b S}{2}\left(1 + \left(\frac{B_d}{P_d}\right)\cos A\right) \tag{1}$$

$$Outer_{ring\,defect\,frequency} = \frac{N_b S}{2}\left(1 - \left(\frac{B_d}{P_d}\right)\cos A\right) \tag{2}$$

$$Ball_{bearing\,defect\,frequency} = \frac{P_d S}{B_d}\left(1 - \left(\frac{B_d}{P_d}\right)^2\cos^2 A\right) \tag{3}$$

$$Cage_{defect\,frequency} = \frac{S}{B_d}\left(1 - \left(\frac{B_d}{P_d}\right)\cos A\right) \tag{4}$$

where N_b is the number of balls, S is speed, B_d is the ball diameter, P_d is the pitch diameter, and A is the contact angle (degrees).

Bearing faults (Figure 2b) can occur for various reasons. Loss or contamination of lubricants is one of the most common causes, as inadequate lubrication leads to increased friction and wear. Shaft misalignment or imbalance often causes uneven loading on the bearing, resulting in accelerated wear and eventual failure. Overload conditions, where the load exceeds the bearing's capacity, can also contribute to premature wear. A shaft voltage that exceeds the insulating capability of the bearing grease can lead to electrical discharge and failure. This voltage often results from the interaction between the rotating magnetic field and stationary components, especially in machines with high switching frequencies or

rapid changes in magnetic fields. Lastly, manufacturing flaws can create weak points in the bearing, making them more susceptible to failure, even under normal operating conditions.

(**a**)

(**b**)
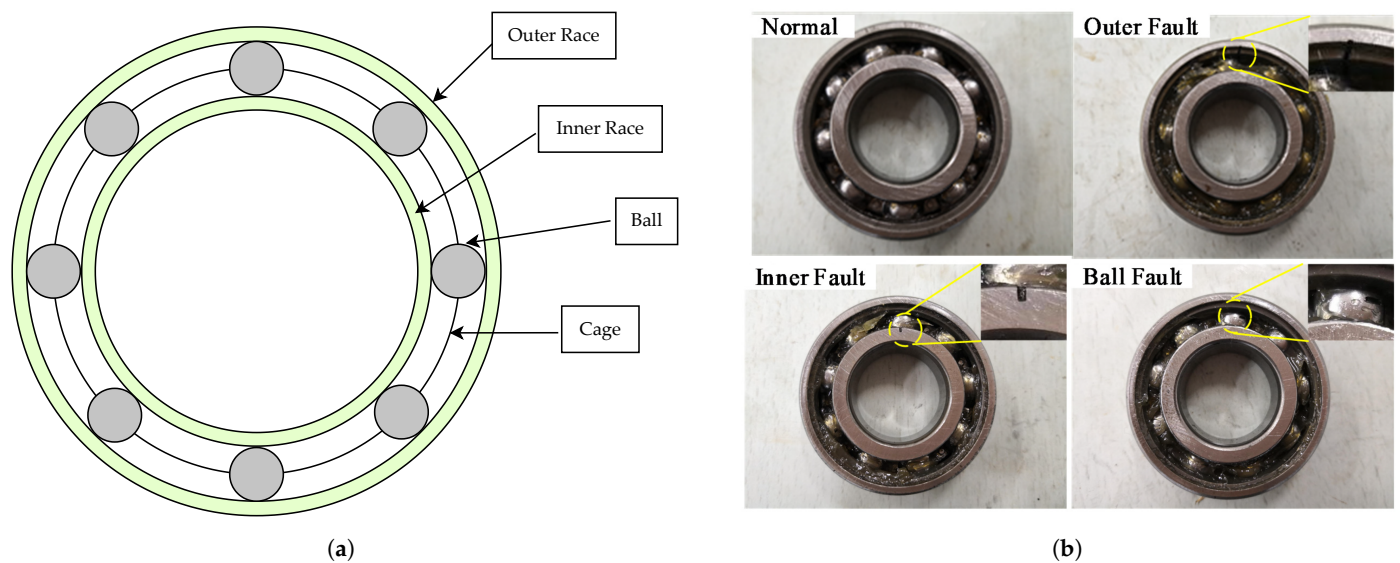
Figure 2. (**a**) Structure of a rolling element bearing. (**b**) The types of faults which can occur in a bearing [23].

2.2. Gear Faults

Gearboxes are of paramount importance in various mechanical systems and industries, due to their versatile and crucial functions [24]. To enable effective operation within preferred speed ranges, gearboxes act as power transmitters, transferring torque and power from a high-speed input to a lower-speed output and vice versa, allowing for operation at both high and low speeds. They also provide precise torque multiplication, direction control, and speed control, to enable machinery to run at the desired speeds and generate the required forces.

Gears are vital across sectors due to their adaptability and customization possibilities, which guarantee top performance, durability, and effective power transfer in a variety of applications [25]. Gearboxes usually operate under a dynamic load or in overload conditions and are prone to suffer from various kinds of defects, such as fatigue pitting, wear, tooth spalling, and tooth fracture [26–29]. In addition, gearboxes are also subjected to impact loads, which are sudden forces or shocks that can occur during operation. These impact loads can exacerbate defects, leading to accelerated wear, structural damage, or even catastrophic failure. A gearbox model is shown in Figure 3a.

Gear faults are interconnected and often evolve from one type to another as damage progresses. Initially, surface and tooth wear can develop due to inadequate lubrication or prolonged friction, leading to gradual material loss [30]. As wear increases, it weakens the surface, making it more susceptible to pitting, where small cavities form due to cyclic loading and fatigue. Over time, these pits can expand and deepen, contributing to surface and tooth spalling, where larger sections of the surface flake off or chip away. If the stress continues to build, it can cause a root crack to form at the base of the gear tooth, which weakens the tooth's structural integrity. This crack can eventually propagate, resulting in a broken tooth. In some cases, exposure to harsh environments can accelerate this deterioration through corrosion, further weakening the gear's surface and exacerbating the effects of wear and spalling.

Gear faults (Figure 3b) can have serious consequences. Dynamic instabilities, such as vibrations, can affect the performance and reliability of a gearbox and the machinery it drives. Fluctuations in load transmitted to the driven machinery can cause uneven wear and reduce the lifespan of components. Impact loads can further intensify these effects,

contributing to increased mechanical stress. Mechanical losses in a power transmission system can lead to reduced efficiency and increased energy consumption. Structural fatigue, caused by repeated stress and impact loads on gearbox components, can eventually lead to mechanical failure if not addressed.
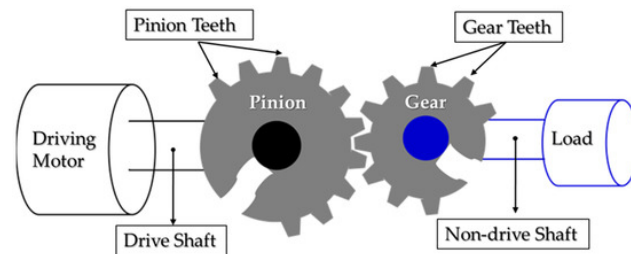
(a)

(b)

Figure 3. (a) A spur gearbox model [31] (b) Fault types in a gear [32].

2.3. Misalignment Faults

A reported 30% of machine downtime in industry is due to poorly aligned machines [33]. There are two types of shaft misalignment faults, which are parallel and angular misalignment. However, a combination of the two can also occur [34]. Shaft misalignment also has some effect on bearings. The alignment condition and the type of coupling used influence the magnitude of the bearing load. In both the horizontal and vertical directions, vibrations tend to be more pronounced in bearings that are farther away from the motor, while those closer to the motor experience less vibrations.

Misalignment faults can occur for several reasons, such as installation errors, thermal expansion, wear and tear, and improper maintenance [21]. Thermal expansion can also cause machine components to shift position, leading to shaft misalignment [29]. Misalignment faults, while less common, can still have significant effects. Incorrect alignment of a drive shaft with the load can cause uneven loading and premature wear on components. When the center of mass does not lie on the axis of rotation, such as with a heavy spot on the rotor [35], this can create an imbalance and lead to vibration and wear. Installation errors, such as improper mounting of bearings or gears, can also cause misalignment and contribute to premature failure. Failure in bearings can be a consequence of misalignment faults, further exacerbating the issue and leading to additional damage. The three types of faults associated with misalignment are shown in Figure 4.

Parallel Misalignment

Angular Misalignment

Combination Misalignment
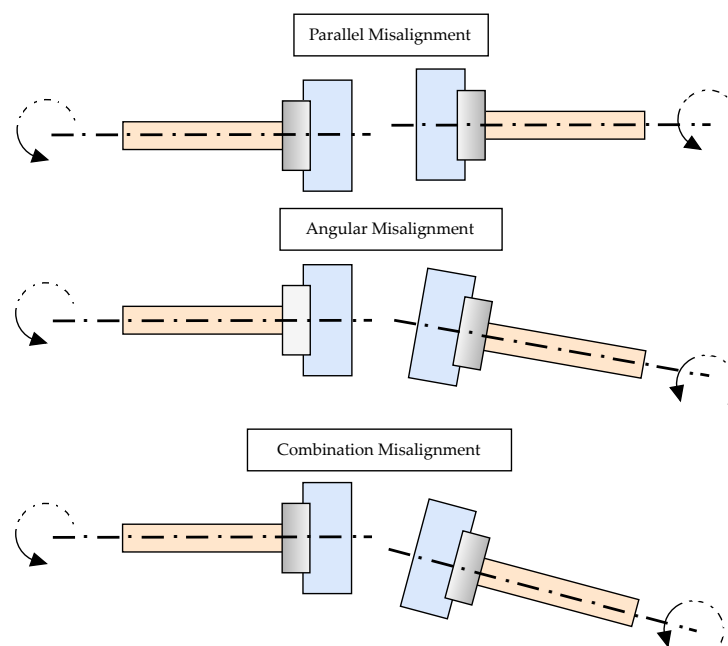
Figure 4. Types of misalignment faults.

3. Fundamentals of RUL Estimation

The core concepts of RUL estimation encompass a comprehensive set of ideas and procedures used to predict the remaining useful life of RMs. This crucial PHM component covers several steps and methods, as discussed in [14]. The first phase, data acquisition, involves gathering data from many sources, including sensor readings and historical information. A system's deterioration patterns are then captured, and degradation modeling approaches are used to comprehend how the system is degrading. Methodologies for feature extraction make it possible to find and choose significant HIs from the received data [6]. Then, diagnostic and prognostic algorithms are used to identify anomalies, categorize fault states, and keep track of the system's health. It should be noted that this review primarily focuses on HI-based methods, due to their ability to condense complex data into simplified, interpretable metrics that directly reflect a system's health status. HI-based models facilitate easier and faster integration into prognostic frameworks and often provide clearer insights into the degradation process. Methods using pre-processed inputs (raw time domain signals or minimally processed data) play a critical role in RUL estimation. In practical scenarios, where capturing detailed signal characteristics is crucial to evade downtime, looking at fully processed information (HIs in particular) is of utmost importance. Nonetheless, several discussions have been presented regarding strategies involving the fusion of these minimally processed signals/data, mainly used in conjunction with data-driven approaches.

In addition, prognostic techniques are used to forecast how degradation will change in the future and to determine how long machinery will continue to be viable. The inherent uncertainty associated with RUL predictions can be expressed and communicated using uncertainty and confidence estimation methods. A variety of RUL prediction methods are used for this process, including data-driven methods like statistical analysis and machine learning, as well as physics-based models that make use of domain expertise and mathematical modeling [36]. Accurate RUL assessment is made possible by a thorough understanding and use of these essential elements, which also improves operational efficiency and allows for well-informed decision-making for asset management or maintenance.

3.1. Data Acquisition

Data acquisition is the first step in prognostics, providing basic condition monitoring information for RUL prediction [7]. It is the process of capturing and storing different

kinds of monitoring data through sensors installed on the respective equipment. The most commonly used sensors for data acquisition are vibration sensors (accelerometers), current sensors, infrared thermometers, temperature sensors, pressure sensors, etc. In practice, the most extensively used data for RUL estimation of mechanical components are vibration data [37]. Run-to-failure data are the most significant when it comes to RUL prediction, as they contain degradation trends for the component. The recorded data are stored at a memory location for further analysis. Figure 5 shows the data acquisition process using wireless devices. The vibration data collected by a sensor are sent through a gateway to a storage location. The data can also be visualized in real time, depending on the type of data acquisition setup used. Advancements in sensor and communication technologies have resulted in the development and use of more complex data acquisition systems in industry. Despite these advances, acquiring high-quality run-to-failure data for machinery remains a difficult task for academic research [7,38]. A systematic review conducted by Lei et al. [7] outlined the following challenges associated with high-quality run-to-failure data acquisition.

- Machine degradation usually spans a considerable duration, progressing gradually from healthy towards failure, which often lasts for several months or even years. Thus, acquiring run-to-failure data for such an extended amount of time poses significant challenges with regard to time and cost.
- Machines are usually not allowed to run to failure in practice, as an unexpected failure may lead to a breakdown or a catastrophic accident, making it difficult to capture run-to-failure data in industrial environments.
- Components such as bearings and gearboxes usually operate under adverse operating conditions. These conditions can include extreme temperatures, high humidity, corrosive substances, abrasive particles, heavy vibrations, high levels of dust or dirt, or exposure to hazardous materials. These interferences are mixed with the data and decrease the quality of data being recorded.
- Most run-to-failure data are captured during non-operational hours or downtime. This results in a huge difference from the operational hour behavior of the machine, reducing the quality of the data.
- Some organizations that can collect run-to-failure data may not publish their data due to privacy reasons or business rivalry.
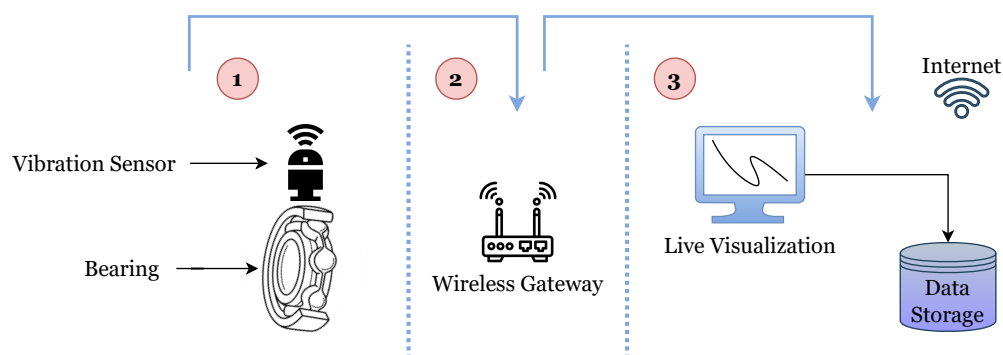
Figure 5. Vibration data acquisition process flow in a nutshell.

Due to the above challenges, most published datasets are acquired from accelerated degradation test beds instead of real industrial equipment. The most frequently used datasets for RUL prediction, which contain run-to-failure data for certain components and that are publicly available, are presented in Table 2. A brief discussion of these datasets is presented below:

1. The Center for Intelligent Maintenance Systems (IMS) dataset includes three sets of bearing data collected for only 1 s each, using vibration sensors at 10 min intervals, except for the first set. For the first set, the first 43 files were collected at 5 min

intervals. All data were collected at a sampling rate of 20.48 kHz. The test involved four bearings, each of which failed at the end of its respective experiment. In test 1, inner race and ball faults occurred in bearings 3 and 4. In test 2, an outer race fault occurred in bearing 1, and similarly, an outer race fault occurred in bearing 3 for test set 3. The data were collected at a constant radial load of 600 lbs and at a constant speed of 2000 revolutions per minute (rpm). In addition, note that the data were collected in a laboratory with natural degradation and not in an industrial environment.

2. The hybrid ceramic bearing dataset experiment was conducted using a 3HP (2.2 kW) AC motor operating at a speed of 1800 rpm. The bearing was subjected to a loading condition of 600 psi (4136.85 kPa), and the setup included both bearing and loading housing. Data were collected at a sampling frequency of 102.4 kHz for 2 s at each sampling point, with intervals of 5 min between sampling points, and the full length of the experiment was approximately 71 h. Two accelerometers were mounted on the bearing housing perpendicular to the shaft, to capture vibration data. The bearings under test consisted of a stainless steel inner race, outer race, and ceramic balls. At the end of the experiment, the bearing was disassembled and photographed.

3. The turbofan engine degradation simulation dataset was generated using the Commercial Modular Aero-Propulsion System Simulation (C-MAPSS). The simulation model contains 14 inputs, which include fuel flow and 13 health parameters, which enable the user to simulate the effects of degradation in the main components of an engine. In total, 21 parameters out of the 58 outputs were used to measure the response of the system under different health and operating conditions. The data have five subsets of data generated under varying operating and health conditions. Under these subsets, 26 columns recorded 21 output parameters, unit number, time (in cycles), and three operational settings. One subset of these data was also used in the PHM challenge in 2008, while the other four were packed into another version.

4. The NASA Glenn Spiral Bevel Gear Dataset focuses on the fatigue strength of gears. The experiment used a closed-loop torque regenerative system to test two sets of spiral bevel gears simultaneously, featuring a 12-tooth pinion and a 36-tooth gear under controlled conditions. A torque of 7500 in-lbs (847.5 Nm) was applied to the gear shaft during the experiment. The pinion and gears were operated at 10,200 rpm and 3400 rpm, with a meshing frequency of 2040 cycles/s. Data were collected to detect pitting damage, a type of fatigue failure. Pitting was categorized into two levels: initial pitting, consisting of pits less than 0.04 cm in diameter covering less than 25% of the tooth contact area, and destructive pitting, consisting of pits greater than 0.04 cm in diameter covering more than 25% of the tooth contact area. Tests were run until initial or destructive pitting occurred, with measurements taken once per minute. Shaft speed, torque, oil debris, and vibration data were captured. Vibration data, sampled at 100 kHz for 2 s intervals, also underwent time synchronous averaging for 113 gear revolutions.

5. The NASA PCoE Batteries dataset includes data from 18,650 lithium-ion batteries tested for charge, discharge, and electrochemical impedance spectroscopy (EIS) profiles at different temperatures. The test setup included a programmable 4-channel DC electronic load and power supply, along with voltmeters, ammeters, thermocouples, custom EIS equipment, and an environmental chamber. Data acquisition was performed at approximately 10 Hz using a PXI chassis-based system and MATLAB control, capturing detailed measurements. Discharge cycles were conducted at various current levels until the battery voltage fell to preset thresholds, including levels below the original equipment manufacturer's recommendation of 2.7 V, to induce deep discharge aging. Tests continued until the batteries reached an end-of-life criterion of 30% capacity fade (2 Ah–1.4 Ah). The dataset includes cycle-level information, with parameters such as operation type, ambient temperature, start time, and detailed measurement data. Parameters recorded during charge and discharge cycles included

the battery voltage, current, temperature, and capacity, while EIS operations included sense current, battery current, current ratio, battery impedance, electrolyte resistance, and charge transfer resistance. This dataset is valuable for developing prognostic algorithms for early battery health and performance assessment.

6. The PRONOSTIA platform collects data from accelerated degradation tests of ball bearings under controlled operating conditions. The data acquisition system utilizes various sensors, including a speed sensor, force sensor, torque sensor, two accelerometers (sampling at 25.6 kHz), and a temperature sensor (RTD probe). All data are aggregated and transmitted to a central unit via a USB 2.0 link for real-time visualization and storage in formatted, time-stamped files. The platform is specifically designed to test bearings under constant speed and load conditions, offering three specific speed and load combinations: 1800 rpm and 4000 Nm, 1650 rpm and 4200 Nm, and 1500 rpm and 5000 Nm. The degradation process is natural, without artificial induction, and the platform is capable of completing tests in a few hours, allowing for multiple experiments within a short time frame. The PRONOSTIA dataset provides valuable data for researchers to test and validate PHM methods, capturing the complete degradation process, offering data under various operating conditions, and providing high sampling rates. However, the dataset is limited to ball bearings, contains varying levels of noise, and may not always align with theoretical models for bearing life prediction. Despite these limitations, PRONOSTIA remains a useful tool for research and development in the field of PHM.

7. The Xi'an Jiaotong University dataset resulted from accelerated degradation tests of rolling element bearings. Fifteen bearings, specifically LDK UER204, were subjected to three different operating conditions of speed and loads (12 kN at 2100 rpm, 11 kN at 2250 rpm, and 10 kN at 2400 rpm). Two accelerometers were mounted on the bearing housing, positioned 90 degrees apart to capture the vibration data. The sampling frequency was 25.6 kHz, with 32,768 samples (1.28 s) recorded every minute. The horizontal accelerometer data were more sensitive to the applied load. The tests ran until the amplitude of the vibration signal exceeded 20 g, which was considered the failure point for the component tested in the dataset. The complete degradation process was characterized by two distinct stages: a normal operating stage with low-level fluctuations, and a degradation stage with increasing vibration amplitudes, making it possible to monitor and predict the remaining useful life of a bearing.

Table 2. Publicly available run-to-failure datasets.

Dataset	Ref.	Sensor
IMS Dataset	[39]	Accelerometer
Hybrid Ceramic Bearing Dataset	[40]	Accelerometer
NASA C-MAPSS/Tuborfan Engine Degradation Dataset	[41]	Simulation data
NASA Glenn Spiral Bevel Gear Dataset	[42]	Accelerometer, Tachometer, Torque sensor
NASA PcoE Batteries Dataset	[43]	Voltmeter, Ammeter, Thermocouple
PRONOSTIA Platform—FEMTO Bearing Dataset	[44]	Accelerometer, Temperature sensor
Xi'an Jiaotong University Dataset	[45]	Accelerometer

3.2. Feature Engineering for Health Indicator (HI) Construction

A HI refers to a measurable parameter or feature that provides information about the health condition or degradation level of a system or component based on certain analyses of long-time recorded data [6,46]. HIs can include various types of signals, measurements, or derived features, such as vibration levels, temperature variations, wear rates, acoustic emissions, power consumption, or other relevant parameters. The study and interpreta-

tion of HIs is critical in determining a system's remaining lifespan, allowing prognosis and maintenance decisions to be made based on the expected amount of degradation or impending failure. This can be utilized to determine the actual health of a component, as well as to detect distinct health phases that a component goes through over its lifetime [47]. It is also considered rare to find a simple and direct HI to track a degradation trend [6].

Figure 6 shows the HI trajectories for three different bearings, consisting of defect frequencies and harmonics. It can be seen that the HI has two distinct phases throughout the degradation trend. These are Phase I, where the component is in its normal operating condition (healthy), and Phase II, where, after a large change in the HI, the component enters a fault mode and starts to degrade exponentially until failure. The limit for failure can be set by the user, depending on their needs. Upon observing the plots above, it can be said that HIs can be instrumental in visualizing degradation trends and also can aid in better RUL estimation compared to directly using raw data.
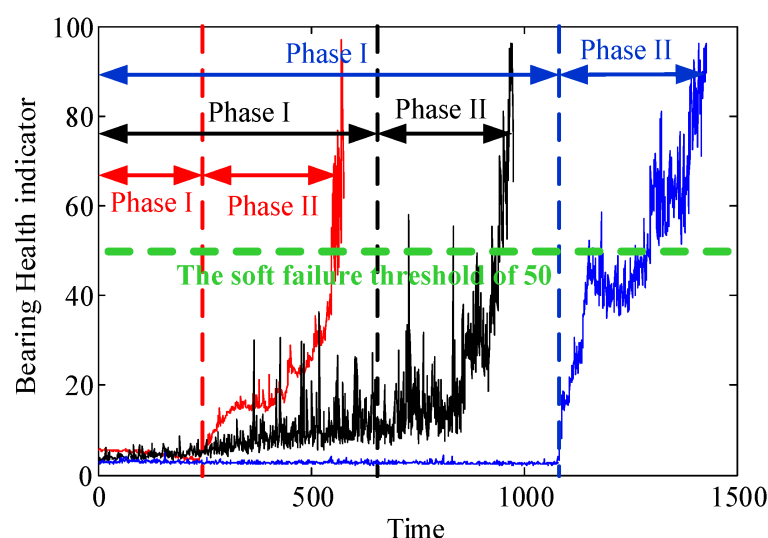

Figure 6. Bearing degradation trajectories [48].

HIs are often developed traditionally through knowledge-based or physics-based techniques, requiring skills or prior understanding of a system, which can be difficult or even impossible to gain at times. In addition, these HIs are usually created for a specific degradation process, making it difficult to generalize them to other processes [49]. As a result, creating a decent HI is a difficult task that, in data-driven methods, relies on sophisticated machine learning techniques capable of extracting HIs automatically from process data [50]. AI-based HIs have gained significant interest recently [51].

In RUL estimation, selecting an HI that demonstrates a strong correlation with the degradation process is essential for accurate predictions. This correlation ensures that the HI reflects a progressive, consistent trend that aligns with a component's wear or fault development, making it a reliable indicator of the remaining life. For instance, HIs such as root mean square (RMS) of vibration or current, root mean square frequency (RMSF), and specific spectral features like kurtosis or crest factor often show strong correlations with fault types, capturing gradual changes in signal energy or frequency content that typically correspond with degradation stages in rotating machinery. However, a major challenge in selecting an HI is establishing a reliable relationship between HIs and actual component degradation, as understanding this connection is inherently complex and often requires specialized experiments and advanced observation techniques. Even when damage levels are measurable, the intricate relationship between HIs and these levels frequently resists straightforward explanation [7].

Selecting or designing an appropriate HI is therefore crucial for accurately identifying both the onset and progression of degradation, particularly in bearings, where an effective HI should strongly correlate with irreversible physical wear. A suitable HI should also

exhibit a steady, consistently increasing or decreasing trend over time, as indicated by metrics such as monotonicity [47]. Evaluating the correlation between an HI and RUL through historical run-to-failure data allows for visualizing degradation trends over time and quantifying their reliability statistically. In cases where single HIs may not fully capture the complexity of degradation, combining multiple indicators can enhance correlation and provide a more comprehensive view of wear and fault patterns.

3.2.1. HI Using Mechanical-Signal-Based Features

Mechanical signal processing plays a crucial role in the identification and analysis of initial anomalies, the extraction of fault-related characteristics, and the development of HIs for bearings and gears [6,52]. Its profound utility stems from its capability to effectively isolate the pertinent components of interest from sources of considerable noise and undesired vibrational elements. After careful pre-processing of a mechanical signal (vibration signal), three conventional feature extraction methods, including time domain, frequency domain, and time–frequency domain, can be used to construct an HI [52].

Time domain techniques: These are directly based on a time waveform to obtain statistical time domain features such as root mean square (RMS), kurtosis, peak, etc. Du et al. [53] used two HIs, RMS and kurtosis of mechanical (vibration) signals, to predict the RUL of bearings. When the kurtosis and RMS of a bearing at a certain time exceed a defined normal interval, it is judged that the bearing enters the degradation stage. Kurtosis, RMS, and skewness are the most commonly used statistical parameters [7]. Cyclic band kurtosis was used in [54] for the diagnosis of incipient faults in rolling element bearings, which is essential for RUL prediction. A similar approach was used in [55], where the authors used highly correlated HIs such as maximum value, RMS, peak-to-peak value, and fast Fourier transformation (FFT) for RUL prediction. These provided better results when compared to state-of-the-art methods such as RMS, Mahalanobis distance of 14 selected temporal features, and principal component analysis (PCA)-based features.

Many studies have used RMS as an HI to study bearing degradation [19,56]. According to [57], RMS can characterize raw degradation data in view of vibration energy. The RMS was filtered using a high-pass filter and then used to construct a bearing HI for the study. Accelerated bearing degradation data were quantified using RMS in [58]. A combined low-pass filter and adaptive line enhancer signal pre-conditioning method was outlined in [59], where RMS, skewness, and kurtosis were calculated from the output of the filter and signal enhancer. Using the above three HIs, accurate information was extracted with regard to the incipient fault stages of bearings. RMS, variance, energy, margin factor, shape factor, Shannon entropy [60], Renyi entropy [61], and Tsallis entropy [62] were fused together to construct a sensitive HI in [63].

Moreover, entropy has been used to successfully detect incipient fault patterns, while variance is only useful towards the final stages of failure [64]. A common issue when using time-domain features was identified in [65]. The efficacy of a data-driven model is significantly influenced by the quality of feature selection when employing statistical signal characteristics as input. Statistical signal features, whether in the temporal or frequency domain, are susceptible to the influence of noise. Moreover, the mere extraction of statistical indicators from the temporal or frequency domain fails to adequately capture the entirety of non-stationary and time-varying features present in bearing signals, thereby unavoidably disregarding pertinent degradation-related information. Table 3 presents time domain features [66,67] as documented in the literature, which are widely utilized for both diagnostic and prognostic purposes.

Table 3. Commonly used time domain features.

Feature	Definition *
Mean	$Mean = \sum \frac{x_i}{N}$
Max value	$Max = max(x)$

Table 3. *Cont.*

Feature	Definition *
Root mean square (RMS)	$RMS = \sqrt{\sum \frac{x_i^2}{N}}$
Square mean root (SMR)	$SMR = \left(\sum \frac{\sqrt{|x_i|}}{N}\right)^2$
Standard deviation (STD)	$STD = \sqrt{\frac{1}{N-1}\sum(x_i - \bar{x})^2}$
Variance	$Variance = \frac{1}{N-1}\sum(x_i - \bar{x})^2$
Crest factor	$Crest\,factor = \frac{max(x)}{\sqrt{\sum \frac{x_i^2}{N}}}$
Latitude factor	$Latitude\,factor = \frac{max(x)}{\left(\sum \frac{\sqrt{|x_i|}}{N}\right)^2}$
Impulse factor	$Impulse\,factor = \frac{max(x)}{\sum \frac{|x_i|}{N}}$
Skewness	$Skewness = \frac{\frac{1}{N}\sum(x_i - \bar{x})^3}{\left[\frac{1}{N-1}\sum(x_i - \bar{x})^2\right]^{\frac{3}{2}}}$
Kurtosis	$Kurtosis = \frac{\frac{1}{N}\sum(x_i - \bar{x})^6}{\left[\frac{1}{N-1}\sum(x_i - \bar{x})^2\right]^{3}}$
Normalized 5th central moment	$5th\,CM = \frac{\frac{1}{N}\sum(x_i - \bar{x})^5}{\left[\frac{1}{N-1}\sum(x_i - \bar{x})^2\right]^{\frac{5}{2}}}$
Normalized 6th central moment	$6th\,CM = \frac{\frac{1}{N}\sum(x_i - \bar{x})^6}{\left[\frac{1}{N-1}\sum(x_i - \bar{x})^2\right]^{3}}$

* N is the total number of the elements of vector x, $\bar{x}$ is the mean, whilst x_i is the ith element.

Frequency domain techniques: This analysis utilizes FFT to convert a time domain signal into the frequency domain. Many fault diagnostics schemes [68–70] utilize FFT as a base technique for analyzing motor currents or vibration signals. Due to the vibration data being non-stationary, there are no obvious features available in the raw data. A unique frequency is seen for different faults in different parts of the component, e.g., a bearing has an inner race fault, outer race fault, etc. Upon using FFT, the raw data can be converted into the frequency domain, where useful information like fault frequencies may be hidden. FFT exhibits certain limitations in its performance, primarily concerning the concealment of distinctive frequencies due to the influence of the supply frequency, as well as its imprecise representation of transient signals [71]. Another major limitation of FFT is that it is unable to correctly distinguish the individual harmonics caused by faults, which can result from either load fluctuations or voltage fluctuations [72]. Apart from Fourier analysis, other approaches are also utilized to extract frequency spectrum features from raw vibration data. Shannon entropy [60], envelope spectrum analysis, spectral skewness, and spectral entropy are other frequency domain feature extraction techniques [73]. Some of the commonly used frequency domain features are tabulated in Table 4.

Table 4. Frequency domain features.

Feature	Definition *
Discrete Fourier Transform	$x(\omega) = \int_{-\infty}^{\infty} x(t)e^{-j\omega t}dt$
Frequency Center	$Frequency\,centre = \sqrt{\frac{\sum_{i=2}^{N}\left(x_i'\right)^2}{4\pi^2 \sum_{i=1}^{N} x_i^2}}$

Table 4. *Cont.*

Feature	Definition *
RMS Frequency	$RMSF = \sqrt{\frac{\sum_{i=2}^{N}\left(x_i'\right)^2}{4\pi^2 \sum_{i=1}^{N} x_i^2}}$
Root Variance Frequency	$RVF = \sqrt{\frac{\sum_{i=2}^{N}\left(x_i'\right)^2}{4\pi^2 \sum_{i=1}^{N} x_i^2} - \left(\frac{\sum_{i=2}^{N}\left(x_i'\right)^2}{4\pi^2 \sum_{i=1}^{N} x_i^2}\right)^2}$

* N is the total number of the elements of vector X, j is the imaginary unit, ω is the angular frequency, whilst x_i is the ith element.

Time–frequency domain techniques: This method explores the characteristics of signals in both the temporal and frequency domains, effectively capturing the evolution of frequency components over time. Prominent examples of time–frequency domain approaches include the short-time Fourier transform (STFT), continuous wavelet transform (CWT), discrete wavelet transform (DWT), Wigner–Ville distribution, and Hilbert–Huang transform [74]. These methods facilitate a comprehensive examination of signal properties by elucidating the dynamics of frequency content regarding temporal variations. These techniques convert one-dimensional time-domain signals into two-dimensional time–frequency functions. Some of the commonly used features are tabulated in Table 5.

Table 5. Commonly used time–frequency domain features.

Feature	Definition *
Short-time Fourier Transform	$STFT_{x(t)}(t,\omega) = \int_{-\infty}^{\infty} x(t)\omega(t-\tau)e^{(-j\omega t)}d\tau$
Continuous Wavelet Transform	$W_{x(t)}(s,\tau) = \frac{1}{\sqrt{s}} \int x(t)\varphi^*\left(\frac{t-\tau}{s}\right)dt$
Discrete Wavelet Transform	$W_{x(t)}(s,\tau) = \frac{1}{\sqrt{2^j}} \int x(t)\varphi^*\left(\frac{t-k2^j}{2^j}\right)dt$
Wavelet Packet Transform	$d_{j+1,2n} = \sum_m h(m-2k)d_{j,n}$
Empirical Mode Decomposition	$x(t) = \sum_{j=1}^{n} c_j + r_n$

* τ = time variable, $\omega(\tau)$ = window function, φ^* = complex conjugate of $\varphi(t)$, J and k are integers, m is no. of coefficients, $d_{j,n}$, $d_{j+1,2n}$ and $d_{j+1,2n+1}$ are wavelet coefficients at sub-bands n, $2n$, $2n + 1$, c_j is jth intrinsic mode function and r_n is residual of data $x(t)$ after extraction of n intrinsic mode functions.

A novel approach for gaining degradation information under cross-operating conditions was proposed in [65]. This method involves constructing a shared latent feature space that spans different operating conditions. The degradation features specific to bearings were extracted in this space. The CWT was used to convert the vibration signals into the time–frequency domain for analysis. Time domain features fused with DWT were used in [75], where the DWT was used as a filter for denoising the time domain features. The proposed method was able to accurately capture the dynamics of the failures. Raw vibration signals were processed using the Hilbert–Huang transform to construct a nonlinear degradation indicator in [74]. A similar approach was taken in [76] to extract new HIs from stationary and non-stationary vibration signals, to track the degradation of the critical components of bearings. One notable drawback of the Hilbert–Huang transform is that its performance is affected when there is non-stationarity in the data flow or variations in the signal dynamics [77].

In summary, this subsection emphasizes the importance of mechanical signal processing in detecting anomalies, extracting fault characteristics, and developing HIs for bearings and gears. Time domain techniques like RMS, kurtosis, and skewness are effective for constructing HIs and characterizing bearing degradation. Frequency domain techniques, including FFT and spectral analysis, convert time domain signals into frequency domain features to reveal hidden fault frequencies, though they face challenges with non-stationary signals. Time–frequency domain techniques, such as STFT, CWT, and DWT, overcome

these challenges by examining the temporal evolution of frequency components, offering a comprehensive analysis of signal properties. The integration of these techniques into a structured framework can improve the accuracy and reliability of RUL estimation for mechanical systems.

3.2.2. HI Using Data-Driven/AI-Based Features

Bearing and gear HIs based on AI techniques require historical data on normal bearing or gear conditions for the training of statistical and probabilistic models. Any deviation (anomaly) observed by the trained model can be considered as a potential degradation starting point. These models can then be used to predict future degradation patterns and estimate the RUL of the components. Continuous monitoring and updating of the models with new data ensures higher accuracy and reliability in the predictions.

It is usually seen that a single HI misses the complete degradation information. Thus, HIs may be integrated with machine learning (ML)-based techniques such as dimensionality reduction to obtain comprehensive information about a degradation trend. PCA can be used as an HI construction technique in this regard. PCA obtains the most significant features in a dataset by reducing its dimensionality whilst preserving the most crucial data, which can be useful to build predictive models. A bearing HI was constructed in [78] by fusing multiple features such as RMS, kurtosis, wavelet energy entropy, and an intrinsic mode function using PCA. In [79], PCA was used to capture the time-varying relationship of process variables and accurately extract weak fault characteristics in the vibration signal, which were used as an HI.

The novelty of this method lies in its innovative approach to bearing RUL estimation, as described in [80], which utilized the textural features of a time–frequency representation (TFR) of data to generate a high-dimensional feature. This feature was subsequently processed through PCA and linear discriminant analysis (LDA) to identify degradation trends in bearings, showcasing the study's unique contribution to the field.

Mahalanobis distance assesses how comparable two data points are based on the covariance structure of the data. It is an anomaly detection technique that can construct HIs from healthy and faulty data. The study conducted in [81] reflected the degradation of bearings by fusing time domain features into one to devise a new HI. Similarly, in [82], fault features were selected by minimum redundancy and maximum relevance and then combined with the Mahalanobis distance to track cooling fan degradation. This was a two-stage method that helped avoid confusion between healthy and degraded data. Many other studies have utilized Mahalanobis distance for prognosis and fault detection purposes [83–85]. In addition, the authors in [86] pre-processed bearing fault signals using empirical mode decomposition and singular value decomposition and then applied Mahalanobis distance to devise an HI.

A recurrent neural network (RNN)-based HI for RUL prediction of bearings was proposed in [87]. An original feature set was formed, comprising eight time–frequency domain features. Using monotonicity and correlation metrics, the most significant features were selected and fed into an RNN to construct the HI. The authors in [74] utilized a convolutional neural network (CNN) to uncover the underlying relationship between vibration data and an HI of the training bearing. This utilization of a CNN harnessed its inherent capabilities in automatic feature extraction. A deep autoencoder (AE) is an effective method for handling high-dimensional data in unsupervised environments [88]. The authors in [89] built an HI for wind turbine defect detection using a denoising AE, which only required healthy data for training. The trained network's reconstruction error from the test data was used to identify the HI. A similar study in [90] learned healthy-state data using a stacked denoising AE, and based on the reconstruction error, an HI for a wind turbine was built.

The advantage of data-driven/AI-based HIs is that, with enough training data, these methods may be used for the majority of RM condition monitoring scenarios, and intelligent monitoring can be accomplished without the use of failure mechanisms or specialized

knowledge, compared to physics- or model-based HIs [88]. Figure 7 provides a full list of the feature engineering techniques that can be used to construct an HI.
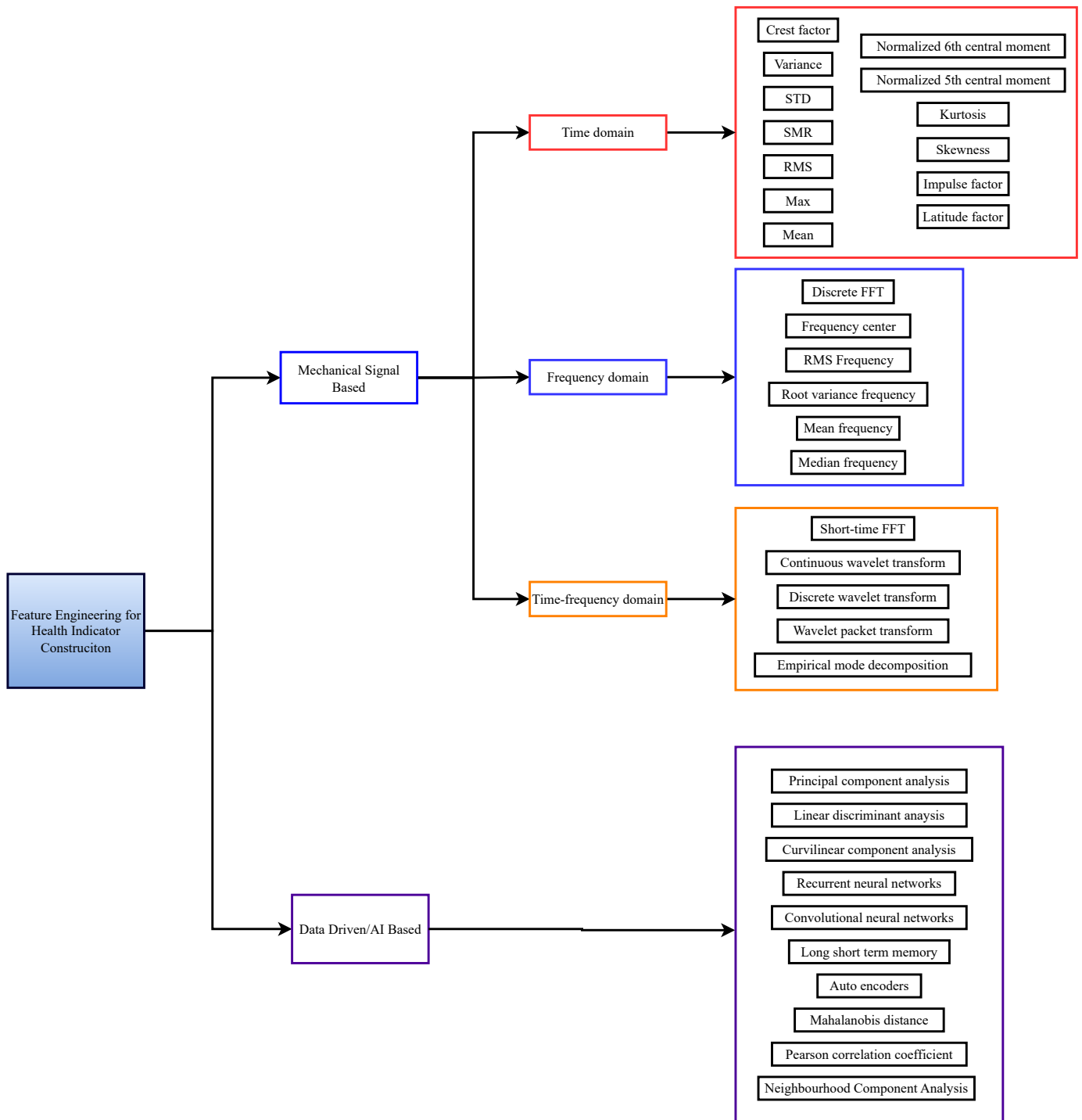
Figure 7. A summary of feature engineering techniques for HI construction.

3.3. Failure Threshold Selection

The determination of an FT is of paramount importance, as it indicates to the user the time when a system passes into a state in which it needs to be repaired or replaced. It also signifies that it will be dangerous to operate the machinery beyond that point. Nowadays, the prevailing approaches employed to determine failure thresholds (FTs) primarily rely on established ISO standards, notably the ISO 20816-3:2022 [91] and ISO/10816 [92] series, or

industry-specific standards like VDI/3834 for wind turbines [7]. These standards, however, solely establish FTs for a limited set of mechanical-signal-based HIs, i.e., RMS and peak values of vibration signals. Unfortunately, there exists a noticeable absence of standardized guidelines for determining FTs for newly devised HIs, particularly those lacking clear-cut physical interpretations.

Typically, an FT is set at a fixed value, often determined as the average HI value across all bearings in a run-to-failure test. Ahmad et al. [19] proposed an adaptive method to determine the FT of a bearing. The method involves utilizing a linear regression model with a gradient threshold based on a window of n RMS values. By continuously updating the window and considering only the most recent RMS samples, this approach adapts to changes in the bearing's degradation behavior. The authors in [74] set the FT to the last value of the HI used to train an e-insensitive support vector regression (e-SVR) model. A similar approach was used to set the FT in [93]. For the HI, RMS values were observed until the bearing under study failed, and the RMS at the point of failure was set as the FT for any new predictions. In addition, the FT was extracted as the value at the final sample of each training dataset in [64], similarly to the previously mentioned studies. Chen et al. [90] used a deep convolutional generative adversarial network (GAN) to create the HI of a wind turbine generator bearing based on reconstruction error to adaptively set a fault failure threshold. The adaptive threshold was set using a deep convolutional generative adversarial network model trained on healthy data. The trained model acted as a self-defined evaluator, automatically generating a threshold based on the output of its discriminator network. This threshold is dynamic and is adjusted based on the model's learned understanding of healthy data, allowing for robust monitoring of wind turbine bearing health. The authors in [94] proposed a method to determine the FT of bearings using vibration signal fluctuations. They applied PCA to identify a degradation indicator and used copula models to analyze its relationship with the peak vibration amplitude. By examining the probability distribution of the vibration features at various degradation levels, they defined the FT as the point where high fluctuations, indicating a potential failure, are likely to occur. Wang et al. [95] set their FT at the time when the HI reached an amplitude of 1. There was no mention of how or why this threshold was selected by the authors. Yang et al. [96] identified a sudden increase in the RMS value of the acceleration signal as the failure point, assuming rapid bearing deterioration. The failure threshold was determined by marking the jump's location and extracting the corresponding HI value at that time.

It must be noted that the determination of an FT is crucial, as it indicates the point at which a system needs repair or replacement and warns against the dangers of continued operation. Despite the importance of FTs, there is a noticeable gap in standardized guidelines for newly developed HIs, especially those lacking clear physical interpretations. The prevailing methods, such as those based on ISO standards or specific industry guidelines like VDI/3834, are primarily focused on mechanical-signal-based HIs like RMS and peak vibration values. Some researchers have set the FT as the average health indicator value across all bearings in a run-to-failure test, or as the last value of the HI used to train models, as in e-insensitive support vector regression. Despite these advancements, there has been relatively little emphasis on FT setup in the literature, highlighting the need for more research in this area. Researchers should focus on developing more robust methods for determining FTs, to enhance the reliability and safety of machinery operations.

3.4. RUL Estimation Techniques

RUL estimation techniques play a crucial role in PHM. These methods are intended to forecast how long a system or component will continue to function, providing proactive maintenance and replacement choices. There are three main RUL estimation strategies, which include model-based techniques, data-driven techniques, and a hybrid of the two [19,97,98].

3.4.1. Model-Based Techniques

Physics-based models replicate the degradation process and estimate RUL using mathematical modeling, physical principles, and domain knowledge. These models focus on deterministic representations of mechanical component degradation based on the underlying physical mechanisms [99]. Modern mechanical systems, on the other hand, have grown substantially in complexity, have highly connected internal components, and frequently operate in harsh conditions with tremendous loads, fluctuating working conditions, and different noise levels [45]. On this account, it is often necessary to integrate statistical methods to account for uncertainties and the stochastic nature of the degradation process. Some exemplary physics-based models have been proposed for RUL estimation, such as the Gamma model [100], the semi-Markov model [101], and the Wiener model [13]. Although these models incorporate stochastic elements, they are grounded in physical principles to describe the degradation process. These techniques have been used in many applications other than prognostics for RMs [102–105].

The extended Kalman filter (EKF), a statistical method, is frequently used in conjunction with physical models for joint parameters and state estimation, particularly for linear systems with unknown parameters. An EKF was proposed in [64] to estimate the degradation of a bearing using time and time–frequency domain features such as entropy and variance. A similar study was conducted in [106] to forecast the RUL of bearings in wind turbines, where a model-based technique based on an enhanced unscented particle filter was used.

Similarly, Wiener processes have gained significant popularity for the characterization of systems undergoing continuous degradation with non-monotonic progressions. This can be attributed to their advantageous mathematical properties and ability to provide meaningful physical interpretations [107]. The degradation processes of systems typically exhibit dissimilarities owing to their distinct operational conditions. Li et al. [108] proposed a method for predicting remaining useful life (RUL) using a Wiener-process-model (WPM) approach that accounts for varying operating conditions. Within this method, a specialized age- and state-dependent WPM was devised to accurately depict the diverse degradation processes observed across different components. A few other studies, refs. [109–111], have also used the WPM for RUL estimation.

In certain instances, degradation processes exhibit a monotonic nature, progressing solely in a singular direction. Examples include wear and fatigue crack propagation in gears. In such scenarios, the Gamma process serves as an appropriate model for degradation processes, wherein the deterioration is presumed to occur gradually over time through a sequence of very small positive increments [11]. A key benefit of utilizing the Gamma process for estimating RUL lies in the simplicity of the mathematical computations and a clear and easily comprehensible physical interpretation.

Shaft and bearing misalignment is a critical issue in the dynamics and condition monitoring of RMs. Real-world systems are complex and unpredictable, and these misalignments are rarely deterministic. Due to fluctuating conditions, wear and tear, and load changes, misalignments often exhibit stochastic variations. Modern modeling techniques have begun to incorporate stochastic or interval uncertainties into misalignment models to accurately capture this variability, as presented in [112]. Stochastic techniques, such as Monte Carlo simulations and probabilistic modeling, simulate the influence of random misalignments, while interval analysis provides a range of possible misalignment scenarios. These uncertainties allow for a more precise evaluation of a system's dynamic behavior under different misalignment conditions, improving the accuracy and reliability of predictive maintenance solutions. More generally, by offering reliable predictions, even in the face of uncertain operating conditions, the inclusion of stochastic and interval uncertainty in the modeling process improves fault diagnostics and prognostics. The significance of incorporating these uncertainties into RUL models has been brought to light by recent advancements in this field, particularly in essential industries, where operational unpredictability or misalignment could lead to major failures or downtime.

Initially, physical modeling was not primarily designed for fault detection, as it lacked an understanding of system behavior in the presence of faults. While physical modeling provides an essential foundation for understanding degradation mechanisms, using it alone is often insufficient, due to the complexity and variability in real-world systems. Physical models are increasingly integrated with statistical approaches to address these limitations, being crucial for capturing the inherent uncertainties and stochastic nature of degradation processes. Dynamic modeling, which involves the continuous representation of system behavior over time, was originally developed for control purposes but has since evolved to incorporate both physical and statistical elements. This integration allows for more accurate predictions of RUL by leveraging the deterministic insights from physical models and the probabilistic strength of statistical models. Regardless, it is widely recognized that fault detection in systems is feasible, as the response of a healthy system differs from that of a faulty system [71]. Although developing accurate degradation models is a difficult process, a combination of physical modeling, statistical approaches, and dynamic modeling can enhance the accuracy of modeling degradation, despite this sometimes being quite complex and rigid due to non-stationarity in the data. In this regard, the complexity of accurately modeling degradation remains a significant challenge, leading to the rise of data-driven techniques for RUL estimation.

Table 6 provides a comprehensive overview of the various physics/model-based techniques integrated with stochastic modeling processes for RUL prediction discussed in this study. It includes information on different methods such as the EKF, WPM, Kalman particle filtering, unscented particle filtering, quadratic regression model, and Kalman filter. Each method is listed alongside its application, year of publication, and the corresponding reference, highlighting their diverse applications, ranging from bearings and turbofan engines to lithium-ion batteries and proton exchange membrane fuel cells.

Table 6. A list of model-based techniques mentioned in this study, with year, application, and publication.

RUL Prediction Method	Application	Year of Publication	Reference
Extended Kalman filter	Bearings	2017	Ref. [64]
		2018	Ref. [113]
		2017	Ref. [17]
Wiener process	Bearings	2017	Ref. [5]
		2023	Ref. [55]
	Turboan engine	2018	Ref. [108]
	Lithium-ion batteries	2020	Ref. [111]
Kalman particle filtering	Bearings	2017	Ref. [58]
Unscented particle filtering	Rotor & bearing systems	2017	Ref. [57]
	Wind turbine bearings	2020	Ref. [106]
	Bearings	2024	Ref. [114]
Quadratic regression model	Bearings	2018	Ref. [19]
Kalman filter	Proton exchange membrane fuel cell	2021	Ref. [104]
	Bearings	2023	Ref. [115]
Gaussian process regression & Wiener process	Bearings	2024	Ref. [116]
Coupled diffusion process & Temporal attention	Bearing	2024	Ref. [117]

3.4.2. Data-Driven Techniques

Regression analysis, ML, DL (DL), and statistical methods are examples of data-driven strategies that use historical data and sensor readings to identify patterns and links between the deterioration process and RUL and that work well for complex mechanical systems. However, they require both healthy and faulty data or run-to-failure data of a system. The deep architectures can extract features automatically instead of having an expert manually create features, as in ML techniques [118–120].

Artificial Neural Networks (ANNs): These networks emulate the intricate workings of the human brain by establishing connections between numerous nodes within a complex layered structure. These networks are widely employed as prominent AI techniques, particularly in the domain of machinery RUL prediction. An ANN model entails a very high computational cost for optimizing the weights of the model [74]. Among the various ANNs, feed-forward neural networks (FNNs) stand out as the prevailing choice in this field [7]. Many studies have utilized FNNs [121,122]. ANNs possess the capability to acquire intricate non-linear relationships through the process of training multi-layer networks. Consequently, they are anticipated to exhibit commendable efficacy in predicting the RUL of complex systems. However, ANNs encounter certain limitations. Primarily, ANNs suffer from reduced transparency, rendering the inner workings of the model less comprehensible. The basic structure of an ANN is shown in Figure 8. Moreover, ANNs typically necessitate substantial quantities of high-quality training data, which can prove challenging to procure within industrial contexts due to noise. Recurrent neural networks (RNNs) are also widely used in RUL prediction, because of their ability to deal with time-series data. ANNs excel in capturing the subtle patterns within data that may be missed by traditional methods. They come with significant computational costs due to the complexity of optimizing their weights.
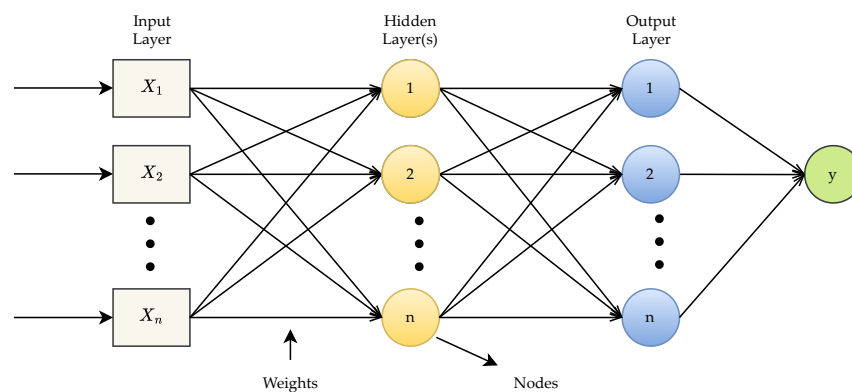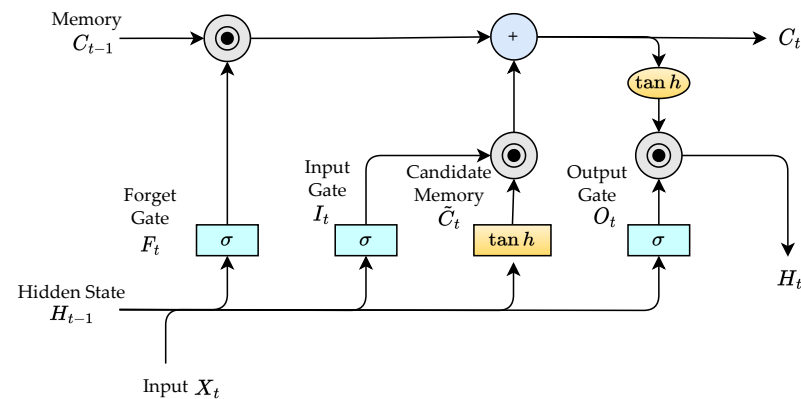

Figure 8. Basic structure of an ANN.

To utilize an ANN for RUL prediction, a few changes need to be made. These include the following: (1) Adjusting the input layer such that it matches the dimensions of the features or the HI derived. (2) Careful configuration of the hidden layers must be performed to capture the complex relationships between the HIs and the RUL. This may lead to the need to experiment with different combinations of hidden layers and numbers of neurons per layer. It is important to consider selecting activation functions, such as ReLU or Tanh, that can introduce non-linearity. Additionally, including dropout layers can help avoid overfitting, especially for smaller datasets. (3) The output layer must be modified to consist of a single neuron that has a linear activation function, to provide a direct mapping from the input features to the predicted continuous value (RUL). In addition, the output may need to be scaled if the target RUL values have not been normalized.

Long Short-term Memory (LSTM) [123,124]: This approach is a variant of RNNs. Data-driven methods often rely on analyzing sensor-based monitoring data, which possess a strong temporal nature, requiring specialized techniques for sequential information handling. RNNs excel in this regard by accepting sequences as input and sequentially performing operations. Consequently, RNNs can effectively comprehend time-series data and prove valuable in addressing RUL prediction challenges. However, traditional RNNs encounter difficulties in capturing long-term dependencies. When confronted with extensive sequential data during training, they may suffer from either vanishing or exploding gradients, leading to sub-optimal training outcomes [125]. To overcome this issue, the LSTM model was proposed. LSTM incorporates two distinct pathways for information processing: one devoted to retaining long-term memory and the other focused on pro-

cessing short-term information, while selectively integrating relevant insights into the former pathway. LSTM employs three gating units, namely an input gate, forget gate, and output gate, to regulate the flow of information within the LSTM unit and control the handling of input data [123]. The basic structure of an LSTM is shown in Figure 9. Sequential data play a crucial role in the prediction of RUL, and to effectively handle such data, numerous frameworks based on RNNs, including RNN, LSTM, and gated recurrent units, have been developed [126,127]. However, RNN-based frameworks, characterized by their recurrent nature, incur a considerable time cost during training and experience performance degradation attributed to long-term dependency.
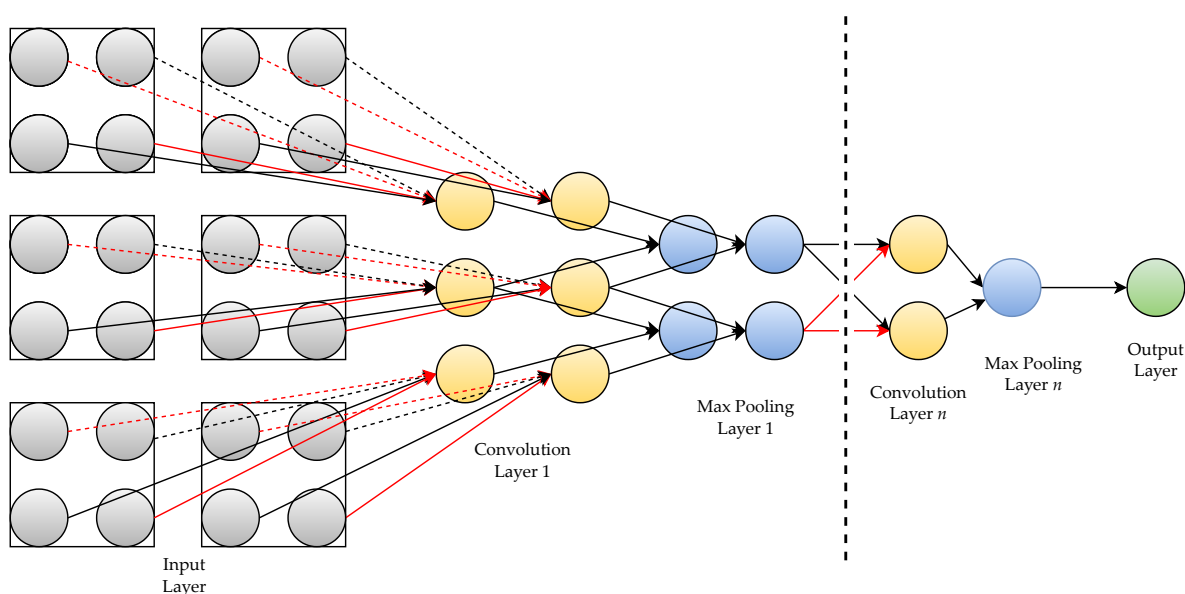
Figure 9. Basic structure of LSTM.

LSTM models offer various advantages, such as their ability to learn long-term dependencies. Long-term dependencies occur when the prediction of an element in the sequence depends on elements that are far away from it in the sequence. FNNs struggle with capturing long-term dependencies because they process each input independently, whereas this is not the case for LSTMs. The vanishing gradient issue is mitigated by employing gating mechanisms, which ensure stable training of such deep networks. The memory cells in LSTM models enable them to preserve information over long sequences, enabling them to selectively retain relevant information while discarding irrelevant details. This makes these models highly effective for tasks where capturing information over long ranges is crucial, such as in time-series prediction for RUL estimation. However, despite their advantages, LSTM networks also come with limitations. These models are more complex than other RNNS, which makes it difficult to understand and implement them at times. Dealing with large datasets may result in increased computational costs, due to this complexity. Another common issue with LSTMs is that they can tend to overfit, especially when they have a complex architecture or are trained on a small dataset. Additionally, it may be difficult to interpret the model, making it difficult to comprehend how it is making its predictions.

To use an LSTM model for RUL estimation purposes, an input layer, one or more LSTM layers, and a dense layer can be used. The input layer should match the shape of the time-series data, followed by an LSTM layer with a favorable number of units. Next, a dropout layer may be used to avoid overfitting. To capture more complex patterns, the LSTM layers may be stacked and then followed by a dropout layer. After these layers, one or more dense layers can be used to learn additional representations from the LSTM layer outputs. Finally, a dense layer can be used containing a single unit and a linear activation function to estimate the RUL. This architecture offers a robust foundation for RUL prediction, striking a balance between model complexity and the ability to generalize effectively from the training data.

Convolutional Neural Network [128,129]. CNNs, as a prominent DL model, have emerged as the dominant approach for solving recognition and detection tasks within the field of computer vision. This model is characterized by three distinct features: local connections, shared weights, and local pooling. These characteristics contribute to CNNs' effectiveness in capturing local patterns and features within images, facilitating their success

in various computer vision applications. CNNs are used to speed up the training process (a drawback for RNNs), but when it comes to time-series forecasting, CNNs run into the same problem: they achieve limited performance for degradation trends. Cheng et al. [74] used a CNN to identify the hidden pattern between a HI and the raw signals, making it possible to automatically estimate the degradation of bearings. A similar study in [130] used a CNN to automatically extract HIs, learn the relationship between degradation and HIs, and predict the RUL. The method was validated using the C-MAPSS dataset for engine degradation. Figure 10 outlines the basic structure of a CNN.
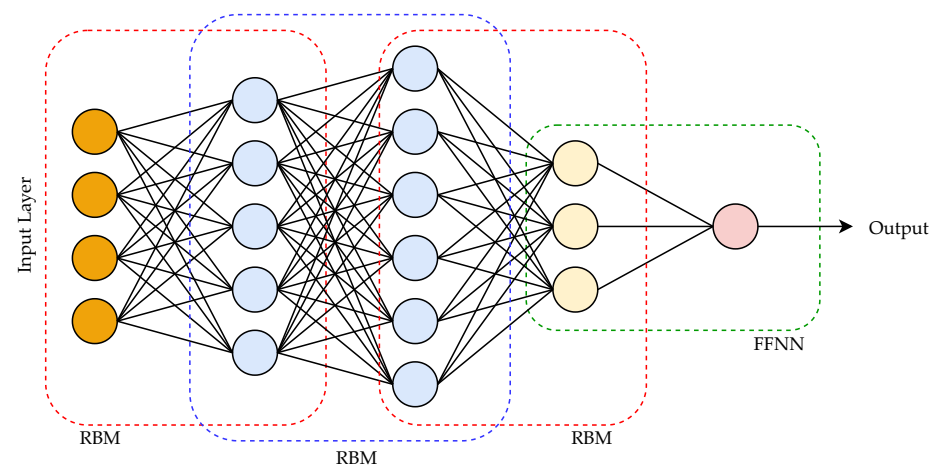

Figure 10. Basic structure of a CNN.

CNNs are effectively able to capture spatial hierarchies and local patterns in data, which may be useful for identifying degradation trends and anomalies related to RUL estimation. CNNs have fewer parameters compared to fully connected networks, due to weight sharing in convolutional layers. This leads to more efficient training and a reduced risk of overfitting. Moreover, these versatile networks are capable of handling multi-dimensional data, such as multi-sensor data, which are often used for RUL estimation. However, CNNs have a few disadvantages when dealing with RUL estimation. These models typically require a huge amount of labeled data to be able to train well, which could be a limitation if the training data are small in size. CNN training is computationally intensive and demands significant computing resources, such as graphic processing units. The design of CNN models often requires extensive experimentation, such as tuning the architecture using various configurations and hyperparameters to achieve the best performance. Standard CNNs may not naturally capture temporal dependencies in time-series data as effectively as models like LSTMs, because they were primarily developed for spatial data. Additionally, non-spatial data may cause CNNs to perform poorly, which limits their usefulness in some RUL estimation settings where capturing sequential dependencies is essential.

To use CNNs for RUL estimation, a basic architecture that includes an input layer, several convolutional layers for feature extraction, pooling layers for dimensionality reduction, and fully connected layers for the final prediction can be used as the starting point. To modify this basic architecture for RUL estimation, the following changes can be made: the addition of more convolutional layers to capture deeper patterns in the data, and utilizing dropout layers to avoid overfitting. Additionally, batch normalization layers can be used to stabilize and accelerate training. Since CNNs may not inherently capture temporal dependencies, a time-distributed approach can be integrated, or the CNN can be combined with LSTM layers to handle temporal aspects. The time-distributed approach in CNNs

applies the same convolutional operations to each time step of a sequence independently, allowing the model to handle sequential data, while preserving the temporal order. Finally, an output layer with a single unit and a linear activation function can be used to estimate the RUL. By making these adjustments, a CNN can be used for more accurate and reliable RUL estimation.

Deep Belief Networks (DBNs): These models are a class of ANNs renowned for their ability to extract features. DBNs commonly combine a stack of serially connected restricted Boltzmann machines (RBMs) [131]. The RBMs are stacked on top of each other, with the output of one serving as the input to the next RBM in the stack, as seen in Figure 11. DBNs are used in a wide range of applications. The earliest application was reported in 2017 [132], where data from multiple sensors were fused for diagnosing bearing faults.

Figure 11. Basic structure of a DBN.

Multiple studies, refs. [133–136], have utilized DBNs for prognosis. Hu et al. [134] used a combination of a DBN and a diffusion process for RUL prediction. The DBN was used as a feature extractor in this case, with locally linear embedding. The study regarding the RUL of aircraft engines in [135] leveraged the feature extraction capabilities of autoencoders and DBNs to model the degradation trend. The developed model was tested using state-of-the-art methods and was observed to be superior, as indicated by the root mean squared error (RMSE) and score indices.

DBNs offer several advantages for RUL estimation. One key benefit is their ability to perform unsupervised pre-training, which helps initialize network weights more effectively and leads to better generalization, particularly with limited labeled data. DBNs are adept at learning hierarchical representations of data, capturing the complex patterns and features essential for accurate RUL estimation. Their generative nature makes them robust to noise, allowing them to handle the noisy sensor data often encountered in industrial settings. Additionally, DBNs can reduce the dimensionality of input data, extracting the most relevant features and improving the efficiency and accuracy of RUL prediction models. The flexibility in the DBN architecture allows for the tailoring of a model to the specific characteristics of a RUL estimation problem, enhancing its adaptability to various types and amounts of sensor data. Despite their advantages, DBNs have several disadvantages in RUL estimation. One significant drawback is their computational complexity and the time-consuming nature of training, especially with large datasets, which can be a constraint in real-time applications. DBNs also require a substantial amount of fine-tuning of hyperparameters, which can be challenging and resource-intensive. Their architecture can become quite complex, making them harder to implement and understand compared to simpler models. Additionally, DBNs can struggle with overfitting, particularly when the amount of labeled data are limited. While they are robust to noise, their performance can degrade if noise levels are extremely high.

Several critical considerations must be taken into account when using DBNs to predict RUL. Firstly, the input layer dimensions should match the feature space of the input data, typically comprising sensor readings or machinery-related features (HIs). Enhancing the DBN's hidden layers may require increasing the number of units or layers to capture intricate data patterns, while avoiding overfitting through techniques such as dropout regularization. Hyperparameter optimization, including tuning the learning rate, momentum, and weight decay, is crucial for improving model performance. Lastly, the output layer should consist of a single unit with a linear activation function to enable the prediction of RUL. These modifications, when systematically applied and fine-tuned, can significantly enhance the DBN's efficacy in accurately predicting RUL in industrial systems.

Time Fusion Transformer (TFT): Transformers are a type of neural network (NN) similar to RNNs or CNNs and that were very recently proposed in [137]. The architecture is an NN structure initially developed for machine translation purposes. It incorporates a self-attention mechanism to capture and model the dependencies between input and output sequences. This self-attention mechanism enables the model to dynamically assign weights to each input element, determining its relative significance in generating the corresponding output [138]. The basic structure of a TFT is shown in Figure 12. In a recent study [139], a transformer neural network was used to predict the RUL of lithium-ion batteries. The transformer encoder was used to learn long-term dependencies of the capacity degradation from battery working records. The transformer layers were a stack of transformer encoders that extracted degradation features from the reconstructed data, with two sub-layers: multi-head self-attention, and feed-forward. This study was a first in this type of application. The fusion model proposed in [140] combines CNN, LSTM, and transformers to improve RUL estimation accuracy for aero-engines. The vanilla transformer model was adapted specifically for RUL estimation by modifying its input and output layers and making additional adjustments to suit aero-engine sensor data. A CNN, LSTM, and their combination layers were integrated into the encoder and decoder layers of the adapted transformer model, resulting in three fusion models.

TFTs offer several advantages for RUL estimation in comparison to traditional methods. TFTs can effectively model temporal dependencies in sequential data, such as sensor readings, by capturing long-range dependencies through self-attention mechanisms. This enables a model to learn complex patterns and relationships in data, potentially leading to more accurate RUL predictions. Additionally, TFTs are highly parallelizable, allowing for efficient training on large datasets. However, TFTs may suffer from high computational costs, especially when dealing with very long sequences or when the model is overly complex. They also require a large amount of data for training, which can be a limitation in applications where data are scarce or expensive to collect. While TFTs offer promising capabilities for RUL estimation, careful consideration of their computational requirements, data availability, and efforts to enhance interpretability is necessary for successful implementation.

Generative Adversarial Network (GAN): The GAN was proposed in 2014 by Goodfellow et al. [141] and has gained popularity very quickly in the field of DL. It involves two distinct parts: a generator and a discriminator. The generator attempts to generate false samples to deceive the discriminator, while the discriminator attempts to discriminate between real and artificially generated data. The structure of the GAN is shown in Figure 13. The GAN falls under the category of generative models, as it contains the ability to create new data based on old data or to simply generate new examples that are similar to the training data [142]. This ability of the GAN can facilitate solving the issue of a lack of data.

Zhang et al. [143] proposed a convolutional recurrent GAN which employed a two-channel fusion convolutional RNN. This was used to self-generate data, to overcome the scarcity of run-to-failure data in a low-cost, quick, and safe manner. The authors tested the proposed model by applying it to three different datasets and obtained a significant drop in estimation errors. A deep adversarial LSTM framework was proposed in [56] for rolling bearing RUL prediction utilizing a two-stage technique. Firstly, the generator predicts

the degradation using the available historical data. In the second stage, the discriminator checks if the degradation is produced from real historical data or is forecast. By carrying out this check, the study minimized the superposition problem of prediction errors. The use of GANs aims to address data scarcity in RUL estimation by increasing the size of the training dataset. Although the RUL of the generated samples might be like the existing data, GANs can introduce subtle variations, enhancing the model's ability to learn a broader range of degradation patterns and improving generalization to new data. Additionally, GAN-generated samples can balance a training dataset by generating data for underrepresented failure modes, leading to better performance across different failure types. This increased data volume also helps mitigate overfitting, a common issue with small datasets, resulting in more accurate RUL predictions.
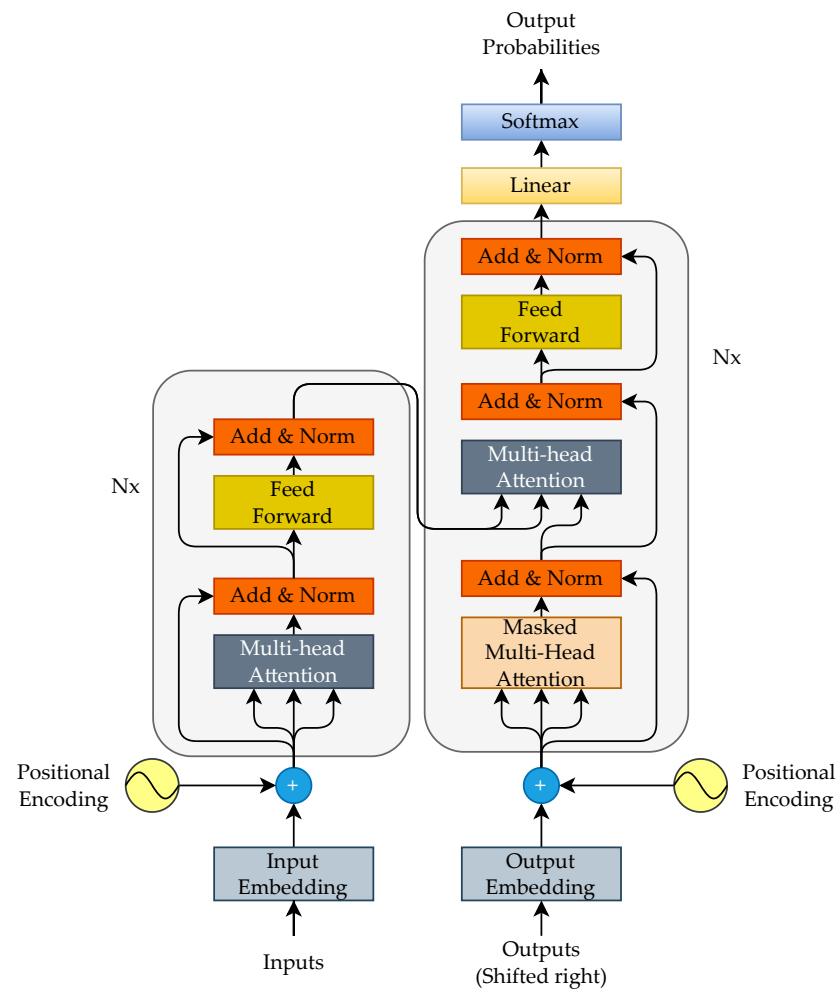

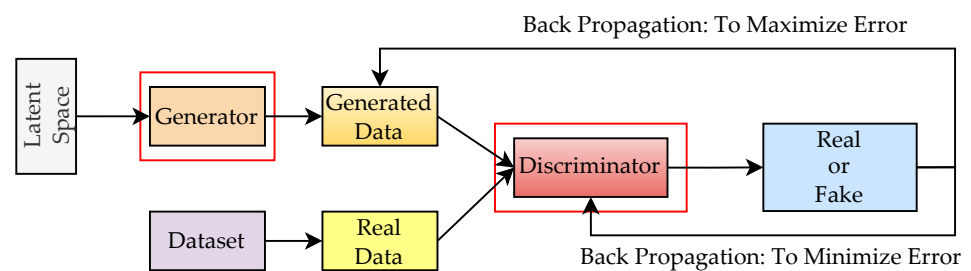**Figure 12.** Basic structure of a transformer.

Figure 13. Basic structure of a GAN.

The main advantage of a GAN is its ability to generate realistic images, signals, and other types of data that may not be easily distinguishable from real data. This property

enables GANs to be used for RUL estimation, as they can generate data that mimics real-world operating conditions and failure modes. This is particularly beneficial in scenarios where labeled data are scarce or challenging to acquire. Through its adversarial training process, a GAN can generate diverse and realistic data, which can enhance the robustness of RUL models. These diverse data expose RUL models to various operating conditions and failure patterns. Additionally, GANs can aid in identifying anomalies in data that may indicate incipient fault stages, thereby enhancing the early detection of faults and the prediction capabilities of RUL models. On the other hand, the training process of GANs is computationally intensive and complex, necessitating high-end computational resources. The quality of generated data must also be validated to ensure that they correctly mimic real-world scenarios, as a poor data quality can lead to potential errors in the prediction process. The integration of synthetic data with existing RUL prediction models and real data must be performed with careful consideration, to avoid problems such as mode collapse and overfitting. Despite these challenges, GANs are a promising tool, due to their potential benefits in enhancing the accuracy and robustness of RUL estimation models.

Traditional data-driven prognostic techniques rely heavily on data from controlled experiments, stress tests, and simulations. These methods assume that such controlled data accurately reflect real-world conditions and failure patterns. However, complex machinery often operates under unpredictable conditions, leading to unexpected deterioration. This conventional approach overlooks the discrepancies between training and real-world data. To address this challenge, transfer learning (TL) has been a widely applied strategy for machine prognostics. TL involves acquiring knowledge by solving a problem where labeled data are abundant and then adapting this knowledge to solve a different but related problem where labeled data are scarce or expensive to obtain, which is the case for most RUL estimation problems. TL is a machine learning technique where a model developed for a particular task is reused as the starting point for a model for a second, related task. This approach leverages the knowledge gained while solving one problem and applies it to a different but related problem, often leading to improvements in performance and a reduction in the time and resources required for training.

The works of [144] state that applying TL for domain adaptation or feature representation transfer enhances the robustness of prognostics in scenarios involving new conditions and unforeseen faults. This approach generalizes insights from a limited set of experimental cases to real-world applications, where equipment operates under varying conditions and encounters new faults. However, using all extracted features indiscriminately in transfer training can yield poor results, highlighting the importance of selecting suitable transferable features. Gu et al. [145] employed TL to address shortcomings in predicting the RUL of lithium-ion batteries. Their article presented a comparison study with traditional methods, identifying a failure to account for variations in battery degradation due to manufacturing differences, environmental factors, and inherent uncertainties, resulting in biased predictive models. To rectify the aforementioned issues, an extreme learning machine (ELM)-based TL was introduced to enhance the predictive accuracy and stability, by addressing variability from arbitrary initial parameters and reducing the training time by eliminating the gradient descent process [146]. According to the results presented, the TL model outperformed other methods in forecasting the RUL of batteries, achieving error reductions of 65.66% when compared to classic ELM models, and 68.89% and 73.95% when compared to alternative approaches.

The consensus self-organizing models (COSMOs) approach, which identifies deviances in equipment using competing representations and identifying outliers, served as the building block for a new TL methodology presented in [147]. The authors further elaborated that using a feature-representation-based TL approach with transferable features addresses the need to adopt prognostic methods for future data samples from unseen distributions and new faults, ensuring robust RUL prediction. This was achieved using transferable features that measure the distance to peers for each sample. The COSMO feature generalizes samples from different domains into a common latent feature space. The experimental

results showed that the proposed approach significantly outperformed traditional methods like transfer component analysis (TCA), correlation alignment (CORAL), and structural correspondence learning (SCL), achieving substantially lower errors in case studies with new operation conditions. Zhang et al. [136] proposed a similar TL method based on COSMO for RUL. Their method only transfers selected features between the source and target domains, without considering their transferability. The study did not obtain a RUL training label according to the bearing degradation trajectory under different working conditions, which may have impacted the accuracy and efficiency of their models. A novel fusion TL strategy that combines LSTM and ELM networks for online bearing RUL estimation is seen in [148]. They used offline bearing vibration signal data as the source domain and online bearing data as the target domain. First, the time-frequency domain features from the source domain were extracted and input into LSTM and ELM networks. These network prediction results had been nonlinearly fused using an ELM network, which were subsequently transferred to online bearing data for RUL prediction. The study reported that the basic LSTM and ELM models limited the prediction accuracy, suggesting that future works refine these network structures for a higher prediction accuracy.

In the field of PHM, TL has demonstrated effectiveness in addressing common rolling bearing issues, including fault detection and diagnosis. Given the inherent consistency in the degradation process of different bearings, TL plays a crucial role in RUL prediction by extracting domain-invariant temporal features and transferring degradation knowledge across various working conditions through domain adaptation [149]. TL significantly reduces the amount of labeled data needed for training by leveraging knowledge from models pre-trained on related tasks. This leads to faster convergence and enhanced performance when dealing with limited or expensive-to-label datasets. TL also allows for a more efficient utilization of computational resources, as it often requires a shorter training time compared to training a model from scratch, which may take a lot of time, depending on the size of the training data and the application. Additionally, TL can enhance generalization capabilities, enabling models to perform better on new, unseen data by transferring learned features and representations that are robust across different domains and tasks. However, a major limitation of transfer learning is the potential for negative transfers, where knowledge from the source domain adversely affects the performance in the target domain, due to significant differences between the two. Selecting an appropriate pre-trained model that closely aligns with the target task is crucial, and this selection process can be non-trivial. Furthermore, TL may lead to suboptimal performance if the source and target domains are too dissimilar. Therefore, utmost care must be taken when selecting a TL model to use for a specific application. Finally, modifying and fine-tuning pre-trained models often requires significant expertise and experimentation, which can be resource-intensive and time-consuming.

A detailed overview of the various data-driven techniques used for RUL prediction, highlighting their application domains, years of publication, and corresponding references, is provided in Table 7. The table categorizes the methods into several groups, including multiobjective DBN, FNNs, DBNs, LSTMs, CNNs, and other advanced techniques, such as deep adversarial LSTMs, transformers, and AEs. Each category lists the specific applications these methods have been applied to, such as turbofan engines, bearings, gears, lithium-ion batteries, and three-phase industrial motors. This tabulated presentation not only demonstrates the diversity and evolution of RUL prediction techniques over time, but also provides a clear reference to the key studies contributing to this field.

Table 7. A list of the data-driven techniques mentioned in this study, with their year, applications, and reference.

RUL Prediction Method	Application	Year of Publication	Reference
Multiobjective DBN	Turbofan engines	2017	Ref. [136]
FNN	Bearings	2018	Ref. [121]
	Three-phase industrial motors	2016	Ref. [122]
DBN	Bearings	2017	Ref. [132]
	Turbofan engines	2022	Ref. [135]
DBN and PF	Bearings	2017	Ref. [40]
Deep CNN	Turbofan engines	2020	Ref. [130]
LSTM	Gears	2020	Ref. [124]
ϵ-SVR	Bearings	2020	Ref. [74]
DBN and RBMs	Bearings	2020	Ref. [134]
Deep adversarial LSTM	Bearings	2021	Ref. [56]
Dual LSTM	Turbofan engines	2021	Ref. [127]
Generalized regression (NN)	Bearings	2021	Ref. [63]
CNN	Bearings	2021	Ref. [65]
		2022	Ref. [98]
	Turbofan engines	2022	Ref. [129]
Gated recurrent unit NN	Bearings	2021	Ref. [93]
Denoising transformer	Lithium-ion batteries	2022	Ref. [139]
Transformer encoder	Bearings	2022	Ref. [18]
Convolutional AE	Bearings	2022	Ref. [118]
Deep Bayesian network	Turbofan engines	2023	Ref. [133]
CNN-LSTM-Transformer	Turbofan engines	2023	Ref. [140]
Deep AE	Bearings	2023	Ref. [120]
Conditional graph convolutional network	Lithium-ion batteries	2024	Ref. [150]
Vision transformer and semi-supervised transfer learning	Lithium-ion batteries	2024	Ref. [151]
Transformer and reweighting technique	Turbofan engines	2024	Ref. [152]
Spatio-temporal convolutional transformer	Bearings	2024	Ref. [153]
Deep reinforcement learning	Bearings	2024	Ref. [154]
Gated Recurrent Units	Bearings	2024	Ref. [155]
Physics-informed multi-state temporal frequency network	Bearings	2024	Ref. [96]

While data-driven methods offer impressive capabilities and find wide application, they often operate as black boxes, hindering our understanding of their decision-making processes. This lack of transparency and interpretability can lead to unreliable predictions when extrapolating beyond the available data. Furthermore, purely data-driven models, despite their ability to fit observed data well, may generate physically inconsistent or implausible predictions when faced with unseen situations, ultimately limiting their generalization performance. There is a growing need to "teach" algorithms by incorporating physical or domain knowledge to address the limitations of black-box ML models. This involves integrating information about governing equations and physical constraints, a concept known as physics-informed learning [156]. This approach promises to enhance the performance and reliability of learning algorithms and is also known as a hybrid of model-based techniques and data-driven techniques.

3.4.3. Hybrid Techniques—A Combination of Physics/Model-Based Techniques and Data-Driven Techniques

Hybrid techniques, which combine model-based approaches with data-driven methods, offer a powerful framework for leveraging the strengths of both paradigms in solving complex problems. Hybrid techniques combine the predictive accuracy and adaptability of data-driven models with the foundational understanding and reliability of physics-based approaches, resulting in more robust and precise RUL estimation.

The study conducted in [157] proposed a hybrid network that utilized a particle filter (PF) and a FNN for RUL prediction. The PF used the Paris–Law model to estimate RUL based on crack growth in railway D-cables dielectric layer, while the FNN was used to learn patterns from data to predict RUL. It must be noted that the study used a weighting scheme to balance the uncertainty and accuracy of each method. The authors in [158] proposed a hybrid model for predicting the RUL of lithium-ion batteries. It combines unscented Kalman filtering (UKF) with relevance vector machine (RVM) regression. The UKF estimates the battery's state and parameters based on a pre-defined model, producing a raw error series. The empirical mode decomposition decomposes this series, isolating the dominant mode representing the error evolution trend. This dominant mode is then used to train the RVM regression model, which predicts the prognostic error. The predicted error is then used to correct the UKF-based RUL prediction.

A similar RVM-based approach was presented in [45]. RVMs with varying kernel parameters are used to identify key degradation points; then, these points are fitted using exponential degradation models. The Fréchet distance, a measure of curve similarity, helps select the optimal degradation model from multiple candidates of curves. This selected model is then extrapolated to predict future degradation and determine the RUL based on a predefined failure threshold. A hybrid method was proposed in [159], where a support vector machine (SVM) is used to classify a bearing's degradation stage into five classes. Then, the method leverages the SVM output to determine whether the bearing is in a low-degradation-rate (LDR) zone or a high-degradation-rate (HDR) zone. For LDR zones, it employs averaging within the corresponding degradation class to smooth the data. However, when the degradation accelerates (HDR zone), it switches to a smoothing algorithm that more precisely tracks the inner relative RMS measurement path, capturing the steeper changes in the HI. An exponentially weighted moving average (EWMA) was combined with support vector regression (SVR) and random forest regression (RFR) for the prediction of RUL in [160]. The EWMA tracks the bearing's degradation over time by monitoring the HI to identify anomalies, and as soon as an anomaly is detected, the SVR and RFR estimate the RUL from that point in time.

Building on these innovative hybrid approaches, there is a growing interest in physics-informed neural networks (PINNs), which integrate physical laws directly into the learning process (see Figure 14) to further enhance the accuracy and reliability of RUL predictions. PINNs were first introduced by Karniadakis et al. in 2019 [161] for solving both forward and inverse problems associated with partial differential equations (PDEs). The PINNs first define the physical laws governing the system using PDEs. Then, a neural network was designed to approximate the solution of these equations. The network's loss function was modified to include physical laws as constraints, meaning it is penalized for both errors in fitting the observed data and for violating the physical constraints. During training, the network learns to adjust its parameters to minimize the loss function, while adhering to the physical laws. This results in a model that accurately captures a system's behavior while adhering to its underlying physics.

Deng et al. [162] proposed a hybrid transfer learning approach for the RUL estimation of bearings. The authors combined a 5-degree-of-freedom model for bearings with a physics-informed Bayesian deep dual network (PI-BDDN), combining a model-based method with a data-driven method. Various failure trajectories are simulated using the physical model, which a PF then calibrates to mimic real-world measurements. Adversarial learning is used by the PI-BDDN to selectively transfer the most relevant knowledge, lever-

aging both simulation data and actual measurements as augmented inputs. The reality gap between simulation and real-world data was addressed by incorporating physical knowledge into the learning process in this study. PINNs were utilized in [163] for wind turbine bearing fatigue prognosis under varying grease qualities. Reduced-order physics models were used for fatigue analysis, while a multi-layer perceptron was used for learning the grease degradation mechanism. These physics-based and data-driven components are integrated into an RNN cell, which updates its state based on the input and previous state, simulating the time-dependent damage accumulation process of a bearing. Liao et al. [164] proposed a method for RUL estimation that combines a graph convolutional network (GCN) with physics-informed training. The GCN learns the spatial relationships between multiple sensors within a system, representing them as a graph structure. The integration of an autoregressive-moving average (ARMA) filter mechanism allows the GCN to learn temporal dynamics and handle dynamic graph topologies, enhancing the model's ability to capture long-term dependencies. Further, the model was trained with a physics-informed loss function that penalizes delayed RUL estimations more than underestimations, reflecting the practical importance of safety over absolute accuracy.
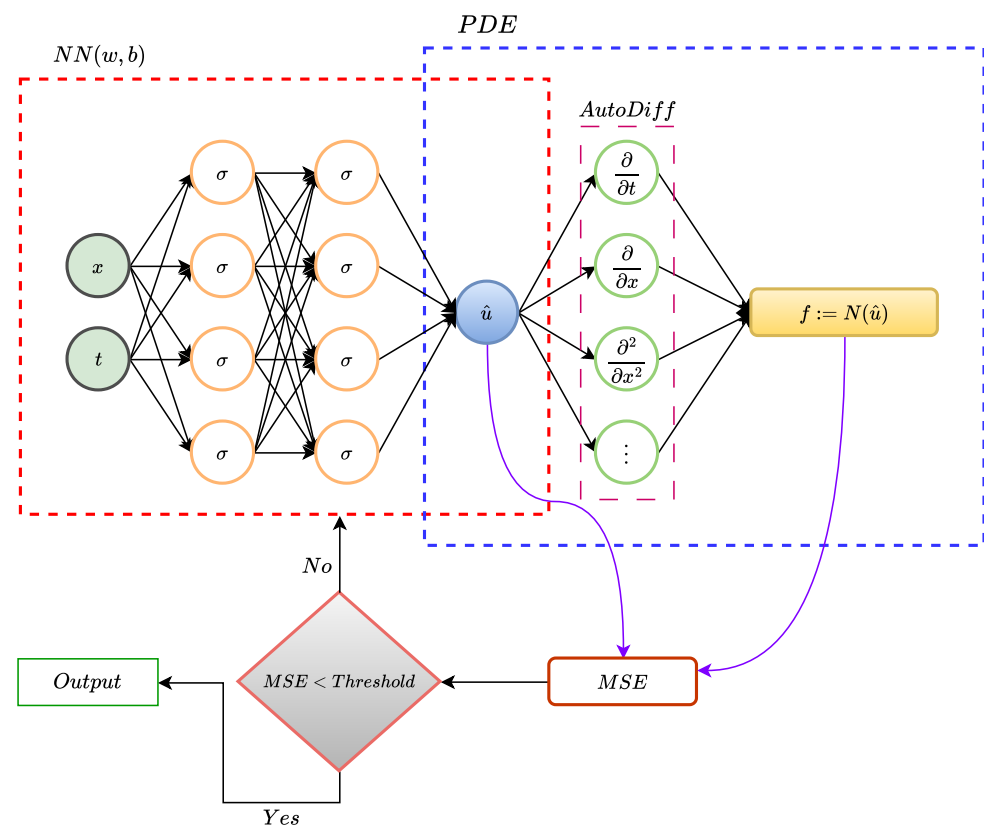
Figure 14. PINN architecture for solving PDEs.

Nascimento et al. [165] presented a PINN that combined a physics-based reduced-order model and a data-driven multi-layer perceptron (MLP) to accurately capture battery discharge behavior and aging. The physics-based model was based on Nernst and Butler–Volmer equations for describing the overall battery discharge, while the MLP modeled the non-ideal voltage. Battery aging was represented by time-dependent internal resistance and available lithium-ion capacity, modeled through an ensemble of variational Bayesian MLPs. Inspired by [165], Fernandez et al. [166] proposed a very similar Bayesian RNN to predict the end-of-discharge (EOD) of lithium-ion batteries. The network was trained using approximate Bayesian computation through subset simulation, which inferred the posterior distribution of the weights, biases, and physical parameters (maximum charge available and internal resistance). A novel physics-informed deep NN, degradation consistency

recurrent neural network (DcRNN) for bearing RUL estimation was presented in [167]. Physical knowledge of monotonic degradation, where the health of a bearing deteriorates over time without recovery, was incorporated into the network. To ensure that the learned features were consistent with the degradation process, a positive increment recurrence relationship was introduced into the network, which integrated monotonic degradation knowledge. The network's final loss function minimized the data loss in the target space and the violations of the physical knowledge in the model outputs.

PINNs offer several key benefits for the field of RUL prediction. PINNs produce more transparent and explainable models than traditional black-box DL approaches by integrating physical constraints. Their inherent physical understanding makes them less prone to overfitting and allows them to generalize better to unseen scenarios. Additionally, PINNs can learn effectively with less labeled data, making them suitable for scenarios where data collection is expensive or time-consuming. Ultimately, PINNs produce predictions that align with a system's underlying physics, leading to more accurate and reliable prognostics. Despite the promising potential of PINNs, there are several challenges to overcome. The design of physics-informed models can be more complex than purely data-driven methods, requiring careful selection of physical constraints and integration strategies. The non-convex nature of the loss function in PINNs can pose challenges during the training process, potentially leading to local optima or instability. Finally, the effectiveness of PINNs is still influenced by the quality of the available data, necessitating data preprocessing techniques to address issues like missing values and noise. Li et al. [156] thoroughly reviewed the emerging field of physics-informed data-driven remaining-useful-life prediction, highlighting its challenges and opportunities for future development.

Building on the detailed information provided in Tables 6 and 7 about individual RUL prediction techniques, Table 8 presents a comprehensive comparison of three approaches used in RUL estimation: model-based techniques, data-driven techniques, and hybrid techniques. The three approaches are summarized in Figure 15. Model-based techniques offer robust predictions, efficient estimation, and high accuracy, but they are costly, time-consuming, and have limited reusability. Data-driven techniques are cost-effective and eliminate the need for physical parameter assumptions. Nevertheless, they are prone to overfitting, require substantial data, and can be inaccurate with high-dimensional data. Hybrid techniques combine the strengths of both approaches, offering improved robustness and adaptability, but they are complex to develop, computationally intensive, and challenging to interpret. Each approach has advantages and disadvantages, highlighting the importance of selecting the most suitable technique based on the specific requirements of the RUL estimation task.

In summary, this subsection delved into the diverse techniques employed for RUL estimation, encompassing model-based, data-driven, and hybrid methods. Model-based techniques rely on physical principles and mathematical models to capture degradation processes, often incorporating stochastic elements to account for uncertainties. While effective for simpler systems, their accuracy can be limited by the complexity of real-world systems and the challenges of modeling non-stationary behavior. Data-driven methods, such as ANNs, LSTMs, CNNs, DBNs, TFTs, and GANs, leverage historical data and sensor readings to identify patterns and predict RUL. These approaches excel in handling complex systems and extracting features automatically, but require significant data availability and may lack transparency and interoperability. Combining model-based and data-driven elements, hybrid techniques present a promising avenue for balancing accuracy and interpretability. These methods utilize physics-based models for a foundational understanding and data-driven models for adaptability and prediction. PINNs are a fascinating area within hybrid techniques, offering greater explainability and consistency with physical laws. Transfer learning has also been explored to leverage pre-trained models and improve the prediction accuracy in new domains. The section outlined the advantages and disadvantages of each approach, highlighting the current state-of-the-art methods and their applications. The

increasing integration of physics-informed approaches within data-driven models promises to lead to more robust and reliable RUL prediction in the future.

Table 8. Advantages and disadvantages of RUL estimation techniques.

Approach	Advantages	Disadvantages
Physics/model-based techniques	• Enables more robust predictions through extrapolation outside of the training data. • Provides efficient and descriptive estimation. • Offers high accuracy and precision. • Estimation of the dynamics of the states at each time interval. • Robustness to limited data	• Costly, consumes a substantial amount of time and computational resources. • Limited reusability. • Modeling complex systems is challenging. • Modeling defects in a stochastic and complex manner presents difficulties. • Sensitive to model errors.
Data-driven techniques	• Low-cost algorithm development and minimal knowledge requirements. • Eliminates the need for assumptions about physical parameters. • Capable of transforming high-dimensional noisy data into lower-dimensional information for prognostic decision-making.	• Over-generalization and over-fitting. • The absence of physical knowledge of the system can lead to counter-intuitive results. • Demands a substantial amount of data. • Low accuracy when dealing with high-dimensional data. • Sensitive to noisy or incomplete data.
Hybrid techniques	• Improved robustness and accuracy by combining different modeling approaches. • Flexibility to adapt to different types of data and system complexities. • Reduced data requirements compared to purely data-driven approaches.	• Complexity of development and implementation. • Higher computational complexity. • Difficulty in interpretation due to model complexity. • No general combination structure.
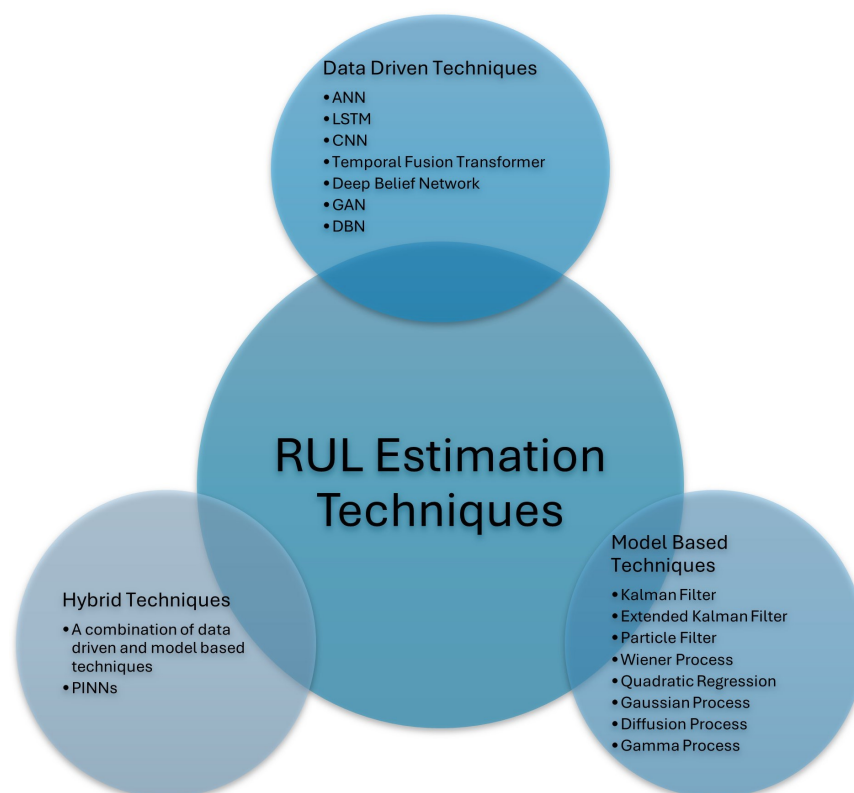
Figure 15. A summarized list of the three types of RUL estimation techniques.

3.5. Hyperparameter Optimization

Hyperparameter optimization is crucial, since it directly impacts the performance, accuracy, and generalization ability of ML and DL models. Properly tuned hyperparameters can make the difference between a model that performs well and one that struggles with overfitting, underfitting, or fails to generalize to new data. Hyperparameter optimization

is essential for maximizing the performance of data-driven approaches, such as ML and DL models like CNNs and LSTMs. In order to avoid overfitting or underfitting and guarantee that a model performs well when applied to unseen data, the procedure entails choosing the optimal set of parameters, such as learning rates or layer depths. Conversely, model-based (physics-based) methods such as EKFs, the Wiener process, and gamma models concentrate on adjusting parameters associated with a system's physical behavior. The optimization procedure must properly calibrate a model to reflect real-world behaviors, and these parameters frequently relate to the physical principles regulating deterioration or failure processes. Lastly, hybrid models leverage the accuracy of physics-based models and the flexibility of machine learning to integrate the best features of data-driven and physics-based approaches. However, because they necessitate balancing the performance of both components, they pose special optimization challenges. The tuning procedure becomes more complicated in hybrid models, since it is crucial to make sure that the predictions made by the data-driven model continue to align with the physical rules that the physics-based model captures. Table 9 presents a summary of the most commonly used hyperparameter optimization techniques.

Table 9. Hyperparameter optimization techniques for different RUL models.

Model Type	Common Hyperparameters	Optimization Techniques
Data-Driven	• Learning rate • Number of hidden layers • Batch size • Dropout rate • Number of epochs • Number of trees, tree depth	• Grid Search: Exhaustive search through all possible combinations of predefined hyperparameter values [168,169]. • Random Search: Randomly selects combinations of hyperparameters [170]. • Bayesian Optimization: Models the objective function to predict promising hyperparameters based on previous evaluations [30,171]. • Hyperband: Efficient resource allocation for hyperparameter tuning, allocating more computation to promising configurations [172].
Model-Based	• Process noise covariance • Measurement noise covariance • Parameters in differential equations • Step size in numerical solutions	• Gradient Descent Methods: Minimizes error between model predictions and observed data [173]. • Expectation-Maximization (EM): Iteratively estimates model parameters. • Simulated Annealing: Probabilistic technique for global optimization in complex models.
Hybrid Models	• Data-driven hyperparameters (learning rate, layers, etc.) • Physics-based parameters (noise covariance, decay rates, etc.) • Weighting factors for combining physics-based and data-driven models	• Evolutionary Algorithms (Genetic Algorithms): Useful for complex, multi-modal search spaces [174]. • Bayesian Optimization: Optimizes both data-driven and physics-based components. • Sequential Model-Based Optimization (SMBO): Builds surrogate models for iterative optimization. • Multi-Objective Optimization: Balances multiple objectives, like minimizing loss while maximizing physical model adherence [175].

3.6. Performance Evaluation

Performance evaluation, also known as validation, is a critical aspect of RUL estimation, where the accuracy and reliability of predictive models are assessed in predicting the lifespan of machinery and components, accounting for both early and late predictions. It involves comparing the predicted values against actual operational data to determine the effectiveness of the estimation methods. By leveraging statistical and machine learning techniques, performance evaluation aims to enhance the precision of RUL predictions. This evaluation is complicated in large-scale, real-world applications, due to the variability of operating conditions, failure modes, and machine types. To handle this complexity, rigorous validation approaches are required to ensure that RUL models remain accurate and generalizable across a wide range of scenarios. A comprehensive discussion of prognostic evaluation metrics can be found in [176].

1. Correlation coefficient: The correlation coefficient aids in establishing a relationship between expected (response) and actual values gained through statistical experiments. The value of the correlation coefficient is always between -1 and $+1$. A similar and identical relationship exists between the two variables if the correlation coefficient value is positive. Otherwise, it shows how different the two variables are from one another. This metric is used to assess the relationship between the HIs and RUL, and not the performance of the prediction model. Assuming x is the HI and y is the RUL, the correlation can be assessed using Equation (5).

$$R = \frac{N(\sum xy) - (\sum x)(\sum y)}{\left[N\sum x^2 - (\sum x)^2\right]\left[N\sum y^2 - (\sum y)^2\right]} \tag{5}$$

2. Root Mean Squared Error (RMSE): The average prediction error of the model is presented as a single value using the RMSE. A better predictive performance is shown by a lower RMSE, since this signifies the model's predictions are more in line with the actual RUL values. On the other hand, a higher RMSE denotes an undesirable model performance and a higher average prediction error.

$$RMSE = \sqrt{\frac{1}{N}\sum_{i=1}^{N}\left(RUL_{predicted} - RUL_{true}\right)^2} \tag{6}$$

3. Mean Absolute Error (MAE): This is useful when measuring absolute error. MAE represents the average absolute prediction error of the model. Even though it is simple to grasp, it is ineffective when data contain extreme values.

$$MAE = \frac{1}{N}\sum_{i=1}^{N}\left|RUL_{predicted} - RUL_{true}\right| \tag{7}$$

4. Mean Squared Error (MSE): The average squared prediction error of the model is presented by the MSE. Similar to RMSE, better predictive performance is shown by a lower RMSE, while a higher RMSE presents an undesirable performance. Although MSE is frequently used, it has the drawback of not being measured in the same units as the expected or measured RUL values, making it challenging to understand an inaccuracy on its own.

$$MSE = \frac{1}{N}\sum_{i=1}^{N}\left(RUL_{predicted} - RUL_{true}\right)^2 \tag{8}$$

5. Coefficient of determination, R^2: This is a statistical measure that indicates how much of the variation in a dependent variable (response) is explained by an independent variable (predictor) in a regression model. The most common interpretation of R^2 is how well the regression model explains the observed data.

$$R^2 = 1 - \frac{\sum\left(RUL_{predicted} - RUL_{true}\right)^2}{\sum\left(RUL_{predicted} - \overline{RUL}\right)^2} \tag{9}$$

6. Prognostic horizon: This identifies whether an algorithm predicts within a specified error margin (specified by the parameter α) around the actual end-of-life and if it does, how much time it allows for any corrective action to be taken [177].

$$PH = EoL - i \tag{10}$$

where

$i = min\{j|(j\epsilon\ell) \wedge (r_*(1-\alpha) \leq r^l(j) \leq r_*(1+\alpha))\}$
ℓ is the set of all time indexes when a prediction is made
l is the index for the lth unit under test
r_* is the ground truth RUL.

In addition, k-fold cross-validation is commonly used to check the reliability of data-driven methods. Here, a model's performance is assessed by dividing run-to-failure data into k subsets, with $k-1$ subsets used for training and the remaining subset for validation, ensuring the model generalizes well to unseen data. However, since RUL estimation relies on time-series data, a rolling or time-based cross-validation approach is often more suitable to preserve temporal dependencies. Time-based cross-validation respects the order of data points, representing the chronological progression of events, unlike traditional k-fold cross-validation, which disrupts this temporal sequence by randomizing subsets.

For time-based cross-validation, a dataset is divided chronologically. In sequential splits, the model is trained on an initial fold and validated on the next in sequence. A growing training window (forward-chaining) takes a similar approach but incrementally expands the training set; for instance, training on Fold 1 and validating on Fold 2, then training on Folds 1 and 2 and validating on Fold 3. Another variation, the rolling window (fixed training window), uses a fixed-size training window that shifts sequentially, training on one period and validating on the next, before moving forward.

Time-based cross-validation provides distinct advantages when evaluating models on time-series data, as it closely simulates real-world settings, where models are trained on historical data to predict future outcomes. This approach prevents data leakage by only using past data for training and future data for validation, ensuring that future information does not inadvertently influence the training process. This method also enhances model generalization by offering a realistic assessment of model performance on future, unseen data, making it a viable approach for time-sensitive tasks like RUL estimation.

Furthermore, both simulation-based and field data approaches can improve the validation of RUL models. When field data are limited, simulation-based validation such as digital twins or physics-based simulations can produce controlled, fictitious settings that closely resemble complex industrial conditions. This allows the accuracy of a model to be evaluated in a range of scenarios. However, field data validation entails evaluating models using experimental data from extensive deployments, where unexpected variability enhances the model's generalizability by revealing any flaws in its predictions.

In summary, assessing the performance of RUL estimation models is a complex procedure that calls for a mix of suitable metrics, validation methods, and practical testing situations. These models can be thoroughly evaluated to guarantee their accuracy, generalizability, and dependability under a variety of real-world circumstances by utilizing time-based cross-validation, field data, and simulation-based validation. These validation techniques are crucial in order to create reliable models that can accurately forecast RUL in intricate industrial applications.

4. Open Problems and Future Prospects

The works mentioned above provide an emphasis on research in the field of the prognostics of RMs. From the review, it can be seen that the prognostics of RMs have made significant progress in the past decade. The traditional approaches for prognosis have their drawbacks in developing an accurate degradation model, due to the substantially increasing complexity of RMs and their components. To mitigate this concern, data-driven methodologies have gained substantial prominence in contemporary practices. However, some open issues remain concerning RUL estimation.

Data-driven techniques have gained great popularity; however, they require degradation data for prediction. The acquisition of run-to-failure data poses significant challenges given the inherent difficulties in capturing and monitoring the complete life cycle of a component until failure occurs, as discussed in Section 3.1. A huge amount of data are

usually required to train data-driven models. Most literature has outlined that the unavailability of real-time run-to-failure data is an issue. These data contain the actual degradation trends of a component's lifetime. Using accelerated degradation data can also give rise to the problem of generalization; therefore, there is a need to acquire data that include all real degradation information. Another important suggestion is to collect data from actual industrial environments. Similarly, another challenge is the imbalance in datasets, where most of the collected data represent the healthy state of the machinery, and very few samples are from the degraded state. This affects the accuracy and reliability of predictive models. Additionally, discrepancies in the probability distribution of data between the training and target domains further complicate model performance. GANs can be used to produce artificial data, which may be able to provide a solution to the scarcity of data in ML applications [142]. By adding fresh samples of data that resemble the existing ones to datasets, GANs can supplement them and avoid overfitting. However, with this possibility comes the risk of failing to capture the full diversity of the training data, leading to the omission of certain modes. As such, to date, this issue remains open, and no general solution has been found.

The generalization issue is a major concern for researchers, relating to a model's ability to make accurate predictions using unseen data or on machines with different ratings and characteristics. Extensive research has been conducted using benchmark datasets, but real-time industrial conditions are continuously changing, causing many AI models to fail in real-time environments [73]. This directly affects the reliability of a developed prognosis model or scheme. To overcome this, feature engineering (HI construction) must be properly conducted [71]. Transfer learning and domain adaptation enable models trained on one domain to adapt to related ones by fine-tuning with target domain data, improving their generalization capabilities. This approach facilitates overcoming generalization issues by transferring knowledge between datasets, such as from laboratory to real-time industrial data. On this basis, a multi-model data fusion combined with deep transfer learning creates a composite health index from multi-channel signals. This improves the characterization of health status and RUL prediction, even when the underlying degradation patterns are complex and nonlinear. While DL models like convolutional neural networks (CNNs) and long short-term memory (LSTM) networks have shown promise for RUL estimation, their complexity often makes them difficult to interpret. The lack of transparency in these models can hinder their adoption for industrial applications, where understanding the decision-making process is crucial. Enhancing model interpretability through techniques such as explainable AI and self-attention maps may make it easier to understand model decisions. Self-attention maps highlight important features within the data, making a model's decision process more transparent and interpretable. In most scenarios, a large transformer-based model can be trained using raw data, after which exploring self-attention maps within the developed network can reveal important decision-making features/HIs. This probing strategy could assist in understanding underlying patterns of degradation, particularly in RMs.

Deploying ML models on hardware in industrial settings presents challenges like ensuring hardware compatibility, minimizing latency, and managing resource limitations. Compatibility concerns involve a model's ability to integrate with the target platform's processing units and architecture, while latency is the delay from input to output, and resource limitations are related to the available memory, computation power, and storage. Addressing these challenges can involve model simplification techniques such as pruning and quantization, utilizing efficient architectures like MobileNets and leveraging edge computing for local data processing. Additionally, model compression and hardware-specific optimizations, including the use of accelerators like GPUs, can significantly enhance performance. Employing a hybrid cloud–edge system could allow for a balance between real-time processing on edge devices and more complex computations in the cloud, ensuring efficient deployment across various applications. Implementing RUL estimation models in real-time industrial settings presents scalability challenges. These models need to efficiently

handle vast amounts of data and provide real-time predictions without significant latency. Developing models that can scale effectively, while maintaining accuracy and speed, is an ongoing area of research.

The accuracy of RUL prediction models is also of concern. One potential solution to this problem is to combine data-driven and physics-based models, utilizing their respective advantages to address the accuracy issue. Data-driven models are excellent at identifying intricate patterns in huge datasets, which enables customization to particular circumstances and degradation patterns. On the other hand, physics-based models provide dependability and the ability to extrapolate beyond the observable data, by offering a fundamental grasp of the underlying failure processes and system behaviors based on physical rules. By combining these two kinds of models, a hybrid strategy may be developed that makes use of the data-driven model's constraints with guidance from the physics-based model, guaranteeing that predictions follow physical laws and are, therefore, more accurate and dependable. By integrating the domain-specific insights of physics-based models with the great flexibility of data-driven approaches, this fusion leads to more robust and precise RUL estimates and improves predictive performance. The abovementioned solution has been applied by many researchers and has been seen to outperform single data-driven or physics-based methods. However, major caveats for this kind of topology include the extra computational complexity, model interpretability, model deployability, data requirements, and incapability of handling uncertainties (this was outlined in Table 8). While the usage of hybrid-based strategies has been remarkable, no general solution that addresses all these challenges simultaneously has been found. Specifically, the increased computational burden can hinder real-time applications, and the complexity of hybrid models often makes them difficult to interpret and deploy in practical settings. Furthermore, these models typically require large and high-quality datasets, which may not always be available. Additionally, many hybrid approaches struggle to effectively quantify and manage uncertainties, which can limit their reliability in unpredictable environments.

Thus, based on the above open problems, future research should further explore the following aspects of the area of prognostics, particularly related to rotating machinery:

- Data Availability, Quality, and Imbalance: Improving real-time run-to-failure data collection using IoT and sensor technology, and sharing anonymized datasets can address data scarcity. Advanced preprocessing, synthetic data generation (GANs), and domain adaptation strategies can enhance model training and accuracy. Addressing data imbalance with techniques like oversampling and adversarial training will improve predictive performance and robustness.

- Deployment on Hardware and Scalability: Advancements in AI-specific hardware, efficient neural network architectures, and edge computing will improve real-time deployment. Hybrid cloud-edge systems will balance processing loads, enhancing scalability and real-time applications. Model simplification and hardware-specific optimizations will ensure compatibility and performance in resource-limited environments.

- Generalization and Interpretability of Models: Future research should focus on developing robust models that generalize well across various industrial settings. Enhanced feature engineering, transfer learning, domain adaptation, and explainable AI techniques can improve model adaptability and transparency. Creating benchmark datasets representing diverse conditions and developing sophisticated feature extraction methods will aid in developing reliable models for real-time applications. Leveraging self-attention maps for interpretability, and the prominence of transfer learning techniques, will ensure accurate RUL predictions and improved predictive performance.

- HI Construction or Feature engineering: For the prognosis of RMs, the mechanical-signal-(vibration signal)-based HIs, specifically time domain features, are the most commonly used, as discussed in Section 3.2, due to their simplicity and reliability. Most HIs have been constructed under normal or constant operating conditions. These HIs can tend to be unreliable when it comes to RUL prediction under varying operating

conditions. Thus, more research should be focused on creating datasets with varying operating conditions and HI construction using them.

- Failure Threshold Selection: FT selection is of major concern. While RUL prediction was performed well in all the literature reviewed, only a few of the authors mentioned the FT at which the prediction should stop or before which the machine or its component should be replaced to prevent unexpected downtime or failures. For data-driven techniques, it was observed that the most common FT is to select the maximum of the HI used for training the model. More emphasis should also be placed on the automatic and adaptive selection of an FT.

RUL estimation methods can be used in industrial settings for power production plants, including thermal, nuclear, and wind facilities, where they will be crucial for the upkeep of vital components like pumps, generators, and turbines. By tracking mechanical degradation processes in these plants, hybrid models that combine data-driven and physics-based methodologies can offer thorough insights into component health. Analyzing vibration data is crucial for spotting wear or structural issues early on. Additionally, comparable predictive maintenance models may be used in the oil and gas sector to keep an eye on the compressors, pumps, and drilling equipment used in both upstream (drilling and exploration) and downstream (refining and distribution) operations. Data-driven methods, including LSTM networks, can evaluate high-frequency vibration data, to provide insights into the health status of RMs and enable prompt actions. In a similar manner, RUL estimation models can be used in water and wastewater treatment facilities, where continuous operation is of utmost importance. These models can be efficient in monitoring the health of the critical equipment in these settings, especially under variable loads and environmental factors. This capability supports reliable water supply and wastewater treatment, while keeping maintenance costs in check, which is particularly important for infrastructure-dependent operations.

Moreover, RUL models are essential for the predictive maintenance of rotating equipment, such as motors, conveyors, gearboxes, and spindles in manufacturing and production lines. These allow optimized maintenance schedules that boost productivity and extend machinery life. RUL models can be used to monitor the condition of heavy machinery such as crushers, conveyor belts, and earth movers in the mining and heavy machinery industries. These models can further be utilized in the transportation sector—spanning railways, aviation, and automotive industries—providing early indicators of wear to prevent in-transit failures and optimize maintenance for fleet operators. These diverse applications across energy and industrial sectors underscore the practical value of RUL estimation and fault detection models, enhancing the reliability, safety, and operational efficiency across various industries.

In conclusion, this review has highlighted significant advancements and persistent challenges in remaining-useful-life (RUL) estimation for RMs. While integrating data-driven and physics-based models shows promise, issues such as data availability, quality, and imbalance remain critical. Future research should focus on enhancing model generalization and interpretability through techniques like GANs, transfer learning, and explainable AI. Additionally, real-time deployment and scalability require advancements in AI-specific hardware and hybrid cloud–edge systems. Addressing these challenges will improve the reliability and applicability of RUL models, enabling timely, cost-effective maintenance and enhanced operational efficiency.

Conflicts of Interest: The authors declare no conflicts of interest.

References

1. Souza, R.; Sperandio Nascimento, E.G.; Miranda, U.; Silva, W.; Lepikson, H. Deep learning for diagnosis and classification of faults in industrial rotating machinery. *Comput. Ind. Eng.* **2020**, *153*, 107060. [CrossRef]
2. Grądzki, R.; Bartoszewicz, B.; Martínez, J.E. Bearing Fault Diagnostics Based on the Square of the Amplitude Gains Method. *Appl. Sci.* **2023**, *13*, 2160. [CrossRef]
3. Vishwakarma, M.; Purohit, R.; Harshlata, V.; Rajput, P. Vibration Analysis & Condition Monitoring for Rotating Machines: A Review. *Mater. Today Proc.* **2017**, *4*, 2659–2664. [CrossRef]
4. Peng, H.; Zhang, H.; Fan, Y.; Shangguan, L.; Yang, Y. A Review of Research on Wind Turbine Bearings' Failure Analysis and Fault Diagnosis. *Lubricants* **2023**, *11*, 14. [CrossRef]
5. Qin, A.; Zhang, Q.; Hu, Q.; Sun, G.; He, J.; Lin, S. Remaining useful life prediction for rotating machinery based on optimal degradation indicator. *Shock Vib.* **2017**, *2017*, 6754968. [CrossRef]
6. Wang, D.; Tsui, K.L.; Miao, Q. Prognostics and Health Management: A Review of Vibration Based Bearing and Gear Health Indicators. *IEEE Access* **2018**, *6*, 665–676. [CrossRef]
7. Lei, Y.; Li, N.; Guo, L.; Li, N.; Yan, T.; Lin, J. Machinery health prognostics: A systematic review from data acquisition to RUL prediction. *Mech. Syst. Signal Process.* **2018**, *104*, 799–834. [CrossRef]
8. Heng, A.; Zhang, S.; Tan, A.C.; Mathew, J. Rotating machinery prognostics: State of the art, challenges and opportunities. *Mech. Syst. Signal Process.* **2009**, *23*, 724–739. [CrossRef]
9. Sikorska, J.Z.; Hodkiewicz, M.; Ma, L. Prognostic modelling options for remaining useful life estimation by industry. *Mech. Syst. Signal Process.* **2011**, *25*, 1803–1836. [CrossRef]
10. Kan, M.S.; Tan, A.C.; Mathew, J. A review on prognostic techniques for non-stationary and non-linear rotating systems. *Mech. Syst. Signal Process.* **2015**, *62*, 1–20. [CrossRef]
11. Si, X.S.; Wang, W.; Hu, C.H.; Zhou, D.H. Remaining useful life estimation—A review on the statistical data driven approaches. *Eur. J. Oper. Res.* **2011**, *213*, 1–14. [CrossRef]
12. Lee, J.; Wu, F.; Zhao, W.; Ghaffari, M.; Liao, L.; Siegel, D. Prognostics and health management design for rotary machinery systems—Reviews, methodology and applications. *Mech. Syst. Signal Process.* **2014**, *42*, 314–334. [CrossRef]
13. Zhang, Z.; Si, X.; Hu, C.; Lei, Y. Degradation data analysis and remaining useful life estimation: A review on Wiener-process-based methods. *Eur. J. Oper. Res.* **2018**, *271*, 775–796. [CrossRef]
14. Zio, E. Prognostics and Health Management (PHM): Where are we and where do we (need to) go in theory and practice. *Reliab. Eng. Syst. Saf.* **2022**, *218*, 108119. [CrossRef]
15. Liang, H.; Cao, J.; Zhao, X. Multibranch and Multiscale Dynamic Convolutional Network for Small Sample Fault Diagnosis of Rotating Machinery. *IEEE Sens. J.* **2023**, *23*, 8973–8988. [CrossRef]
16. Rajabi, S.; Azari, M.S.; Santini, S.; Flammini, F. Fault diagnosis in industrial rotating equipment based on permutation entropy, signal processing and multi-output neuro-fuzzy classifier. *Expert Syst. Appl.* **2022**, *206*, 117754. [CrossRef]
17. Singleton, R.K.; Strangas, E.G.; Aviyente, S. The use of bearing currents and vibrations in lifetime estimation of bearings. *IEEE Trans. Ind. Inform.* **2016**, *13*, 1301–1309. [CrossRef]
18. Guo, D.; Cao, Z.; Fu, H.; Li, Z. Remaining Useful Life Estimation for Rolling Bearings Using MSGCNN-TR. *IEEE Sens. J.* **2022**, *22*, 24333–24343. [CrossRef]
19. Ahmad, W.; Khan, S.A.; Kim, J.M. A hybrid prognostics technique for rolling element bearings using adaptive predictive models. *IEEE Trans. Ind. Electron.* **2017**, *65*, 1577–1584. [CrossRef]
20. Jin, X.; Zhou, W.; Ma, J.; Su, H.; Liu, S.; Gao, B. Analysis on the vibration signals of a novel double-disc crack rotor-bearing system with single defect in inner race. *J. Sound Vib.* **2024**, *595*, 118729. [CrossRef]
21. Peng, B.; Bi, Y.; Xue, B.; Zhang, M.; Wan, S. A Survey on Fault Diagnosis of Rolling Bearings. *Algorithms* **2022**, *15*, 347. [CrossRef]
22. Wu, G.; Yan, T.; Yang, G.; Chai, H.; Cao, C. A review on rolling bearing fault signal detection methods based on different sensors. *Sensors* **2022**, *22*, 8330. [CrossRef] [PubMed]
23. Liu, S.; Xie, J.; Shen, C.; Shang, X.; Wang, D.; Zhu, Z. Bearing fault diagnosis based on improved convolutional deep belief network. *Appl. Sci.* **2020**, *10*, 6359. [CrossRef]
24. Ren, H.; Dai, Z.; Zhou, B.; Zhang, B.; Yin, A.; Pei, L.; Cao, Q. Vibration Monitoring and Semisupervised Multivariate Invertible Deep Probabilistic Learning for Gearbox Faults Identification. *IEEE Sens. J.* **2022**, *22*, 22020–22029. [CrossRef]
25. Cirrincione, G.; Kumar, R.R.; Mohammadi, A.; Kia, S.H.; Barbiero, P.; Ferretti, J. Shallow versus deep neural networks in gear fault diagnosis. *IEEE Trans. Energy Convers.* **2020**, *35*, 1338–1347. [CrossRef]
26. Li, Q.; Ji, X.; Liang, S.Y. Incipient fault feature extraction for rotating machinery based on improved AR-minimum entropy deconvolution combined with variational mode decomposition approach. *Entropy* **2017**, *19*, 317. [CrossRef]
27. Li, J.; Yao, X.; Wang, H.; Zhang, J. Periodic impulses extraction based on improved adaptive VMD and sparse code shrinkage denoising and its application in rotating machinery fault diagnosis. *Mech. Syst. Signal Process.* **2019**, *126*, 568–589. [CrossRef]
28. Shao, H.; Lin, J.; Zhang, L.; Galar, D.; Kumar, U. A novel approach of multisensory fusion to collaborative fault diagnosis in maintenance. *Inf. Fusion* **2021**, *74*, 65–76. [CrossRef]

29. Guo, Y.; Jiang, S.; Yang, Y.; Jin, X.; Wei, Y. Gearbox fault diagnosis based on improved variational mode extraction. *Sensors* **2022**, *22*, 1779. [CrossRef]

30. Kumar, S.; Raj, K.K.; Cirrincione, M.; Cirrincione, G.; Kumar, R.R. Gear Degradation Study using Statistical Time Features and Shallow Neural Networks. *IEEE Access* **2024**, *12*, 111411–111421. [CrossRef]

31. Nguyen, C.D.; Prosvirin, A.; Kim, J.M. A reliable fault diagnosis method for a gearbox system with varying rotational speeds. *Sensors* **2020**, *20*, 3105. [CrossRef] [PubMed]

32. Jiao, J.; Zhao, M.; Lin, J.; Zhao, J. A multivariate encoder information based convolutional neural network for intelligent fault diagnosis of planetary gearboxes. *Knowl.-Based Syst.* **2018**, *160*, 237–250. [CrossRef]

33. Gurav, S.; Waquas, K.; Yusuf, K.; Akash, J.; Meiraj, B.; Mumbai, N.; Ospanova, A. Analysis of Study of Effect of Misalignment on Rotating Shaft. *Int. J. Innov. Res. Sci. Eng. Technol.* **2022**, *11*, 3877–3880.

34. Ab Ghani, A.F.; Razali, M.; Zainal, Z.; Febrian, I. Detection of Shaft Misalignment Using Machinery Fault Simulator (MFS). *J. Adv. Res. Appl. Sci. Eng. Technol.* **2016**, *4*, 47–57.

35. Zhou, W.; Jin, X.; Ding, L.; Ma, J.; Su, H.; Zhao, A. Research on vibration signal decomposition of cracked rotor-bearing system with double-disk based on CEEMDAN-CWT. *Appl. Acoust.* **2025**, *227*, 110254. [CrossRef]

36. Ferreira, C.; Gonçalves, G. Remaining Useful Life prediction and challenges: A literature review on the use of Machine Learning Methods. *J. Manuf. Syst.* **2022**, *63*, 550–562. [CrossRef]

37. Li, H.; Li, Y.; Yu, H. A novel health indicator based on cointegration for rolling bearings' run-to-failure process. *Sensors* **2019**, *19*, 2151. [CrossRef] [PubMed]

38. Hendriks, J.; Dumond, P.; Knox, D. Towards better benchmarking using the CWRU bearing fault dataset. *Mech. Syst. Signal Process.* **2022**, *169*, 108732. [CrossRef]

39. Qiu, H.; Lee, J.; Lin, J.; Yu, G. Wavelet filter-based weak signature detection method and its application on rolling element bearing prognostics. *J. Sound Vib.* **2006**, *289*, 1066–1090. [CrossRef]

40. Deutsch, J.; He, M.; He, D. Remaining useful life prediction of hybrid ceramic bearings using an integrated deep learning and particle filter approach. *Appl. Sci.* **2017**, *7*, 649. [CrossRef]

41. Saxena, A.; Goebel, K.; Simon, D.; Eklund, N. Damage Propagation Modeling for Aircraft Engine Run-to-Failure Simulation. In Proceedings of the 1st International Conference on Prognostics and Health Management (PHM08), Denver, CO, USA, 6–9 October 2008. [CrossRef]

42. Dempsey, P.J.; Wade, D.R.; Antolick, L.J.; Thomas, J. *Investigation of Spiral Bevel Gear Condition Indicator Validation via AC-29-2C Using Fielded Rotorcraft HUMS Data*; Technical Report; NASA: Pasadena, CA, USA, 2014.

43. Li-Ion Battery Aging Datasets | NASA Open Data Portal—data.nasa.gov. Available online: https://data.nasa.gov/dataset/Li-ion-Battery-Aging-Datasets/uj5r-zjdb?category=dataset&view_name=Li-ion-Battery-Aging-Datasets (accessed on 20 September 2024).

44. Nectoux, P.; Gouriveau, R.; Medjaher, K.; Ramasso, E.; Chebel-Morello, B.; Zerhouni, N.; Varnier, C. PRONOSTIA: An experimental platform for bearings accelerated degradation tests. In Proceedings of the PHM'12—IEEE International Conference on Prognostics and Health Management, Denver, CO, USA, 18–21 June 2012; pp. 1–8.

45. Wang, B.; Lei, Y.; Li, N.; Li, N. A Hybrid Prognostics Approach for Estimating Remaining Useful Life of Rolling Element Bearings. *IEEE Trans. Reliab.* **2020**, *69*, 401–412. [CrossRef]

46. Jiao, R.; Peng, K.; Dong, J.; Zhang, K.; Zhang, C. A Health Indicator Construction Method based on Deep Belief Network for Remaining Useful Life Prediction. In Proceedings of the 2019 Prognostics and System Health Management Conference (PHM-Qingdao), Qingdao, China, 25–27 October 2019; pp. 1–6. [CrossRef]

47. Duong, B.P.; Khan, S.A.; Shon, D.; Im, K.; Park, J.; Lim, D.S.; Jang, B.; Kim, J.M. A reliable health indicator for fault prognosis of bearings. *Sensors* **2018**, *18*, 3740. [CrossRef] [PubMed]

48. Li, Q.; Liang, S.Y. Intelligent prognostics of degradation trajectories for rotating machinery based on asymmetric penalty sparse decomposition model. *Symmetry* **2018**, *10*, 214. [CrossRef]

49. LeCun, Y.; Bengio, Y.; Hinton, G. Deep learning. *Nature* **2015**, *521*, 436–444. [CrossRef]

50. González-Muñiz, A.; Díaz, I.; Cuadrado, A.A.; García-Pérez, D. Health indicator for machine condition monitoring built in the latent space of a deep autoencoder. *Reliab. Eng. Syst. Saf.* **2022**, *224*, 108482. [CrossRef]

51. Goebel, K.; Celaya, J.; Sankararaman, S.; Roychoudhury, I.; Daigle, M.; Saxena, A. *Prognostics: The Science of Making Predictions*; CreateSpace Independent Publishing Platform: North Charleston, SC, USA, 2017.

52. Wu, B.; Li, W.; Qiu, M.q. Remaining useful life prediction of bearing with vibration signals based on a novel indicator. *Shock Vib.* **2017**, *2017*, 8927937. [CrossRef]

53. Du, W.; Hou, X.; Wang, H. Time-varying degradation model for remaining useful life prediction of rolling bearings under variable rotational speed. *Appl. Sci.* **2022**, *12*, 4044. [CrossRef]

54. Borghesani, P.; Pennacchi, P.; Chatterton, S. The relationship between kurtosis-and envelope-based indexes for the diagnostic of rolling element bearings. *Mech. Syst. Signal Process.* **2014**, *43*, 25–43. [CrossRef]

55. Liu, Q.; Zhang, Y.; Si, X.; Fan, Z. DLVR-NWP: A Novel Data-Driven Bearing Degradation Model for RUL Estimation. *IEEE Trans. Instrum. Meas.* **2023**, *72*, 3508309. [CrossRef]

56. Lu, B.L.; Liu, Z.H.; Wei, H.L.; Chen, L.; Zhang, H.; Li, X.H. A Deep Adversarial Learning Prognostics Model for Remaining Useful Life Prediction of Rolling Bearing. *IEEE Trans. Artif. Intell.* **2021**, *2*, 329–340. [CrossRef]

57. Tse, P.W.; Wang, D. State space formulation of nonlinear vibration responses collected from a dynamic rotor-bearing system: An extension of bearing diagnostics to bearing prognostics. *Sensors* **2017**, *17*, 369. [CrossRef] [PubMed]

58. Lei, Y.; Li, N.; Lin, J. A New Method Based on Stochastic Process Models for Machine Remaining Useful Life Prediction. *IEEE Trans. Instrum. Meas.* **2016**, *65*, 2671–2684. [CrossRef]

59. Kosasih, B.Y.; Caesarendra, W.; Tieu, K.; Widodo, A.; Moodie, C.A.; Tieu, A.K. Degradation trend estimation and prognosis of large low speed slewing bearing lifetime. *Appl. Mech. Mater.* 2014, *493*, 343–348. [CrossRef]

60. Wu, J.; Wu, C.; Cao, S.; Or, S.W.; Deng, C.; Shao, X. Degradation Data-Driven Time-To-Failure Prognostics Approach for Rolling Element Bearings in Electrical Machines. *IEEE Trans. Ind. Electron.* **2019**, *66*, 529–539. [CrossRef]

61. He, M.; Guo, W. An Integrated Approach for Bearing Health Indicator and Stage Division Using Improved Gaussian Mixture Model and Confidence Value. *IEEE Trans. Ind. Inform.* **2022**, *18*, 5219–5230. [CrossRef]

62. Liu, Y.; Wang, F.; Chang, Y.; Gao, F.; He, D. Performance-relevant kernel independent component analysis based operating performance assessment for nonlinear and non-Gaussian industrial processes. *Chem. Eng. Sci.* **2019**, *209*, 115167. [CrossRef]

63. Yang, C.; Ma, J.; Wang, X.; Li, X.; Li, Z.; Luo, T. A novel based-performance degradation indicator RUL prediction model and its application in rolling bearing. *ISA Trans.* **2022**, *121*, 349–364. [CrossRef]

64. Singleton, R.K.; Strangas, E.G.; Aviyente, S. Extended Kalman Filtering for Remaining-Useful-Life Estimation of Bearings. *IEEE Trans. Ind. Electron.* **2015**, *62*, 1781–1790. [CrossRef]

65. Wang, X.; Wang, T.; Ming, A.; Zhang, W.; Li, A.; Chu, F. Cross-Operating Condition Degradation Knowledge Learning for Remaining Useful Life Estimation of Bearings. *IEEE Trans. Instrum. Meas.* **2021**, *70*, 1–11. [CrossRef]

66. Ferretti, J.; Barbiero, P.; Randazzo, V.; Cirrincione, G.; Pasero, E. Towards Uncovering Feature Extraction From Temporal Signals in Deep CNN: The ECG Case Study. In Proceedings of the 2020 International Joint Conference on Neural Networks (IJCNN), Glasgow, UK, 19–24 July 2020; pp. 1–7. [CrossRef]

67. Kumar, S.; Buksh, N.; Raj, K.K.; Kumar, R.R. A Comparative Classification Study for Broken Rotor Bar Fault and its Severity Analysis using Machine Learning Approaches in Rotating Machines. In Proceedings of the 2023 IEEE International Conference on Energy Technologies for Future Grids (ETFG), Wollongong, Australia, 3–6 December 2023; IEEE: New York, NY, USA, 2023; pp. 1–6. [CrossRef]

68. Antonino-Daviu, J.; Riera-Guasp, M.; Pons-Llinares, J.; Park, J.; Lee, S.B.; Yoo, J.; Kral, C. Detection of Broken Outer-Cage Bars for Double-Cage Induction Motors Under the Startup Transient. *IEEE Trans. Ind. Appl.* **2012**, *48*, 1539–1548. [CrossRef]

69. Yang, T.; Pen, H.; Wang, Z.; Chang, C.S. Feature Knowledge Based Fault Detection of Induction Motors Through the Analysis of Stator Current Data. *IEEE Trans. Instrum. Meas.* **2016**, *65*, 549–558. [CrossRef]

70. Maruthi, G.S.; Hegde, V. Application of MEMS Accelerometer for Detection and Diagnosis of Multiple Faults in the Roller Element Bearings of Three Phase Induction Motor. *IEEE Sens. J.* **2016**, *16*, 145–152. [CrossRef]

71. Kumar, R.R.; Andriollo, M.; Cirrincione, G.; Cirrincione, M.; Tortella, A. A comprehensive review of conventional and intelligence-based approaches for the fault diagnosis and condition monitoring of induction motors. *Energies* **2022**, *15*, 8938. [CrossRef]

72. Karmakar, S.; Chattopadhyay, S.; Mitra, M.; Sengupta, S.; Karmakar, S.; Chattopadhyay, S.; Mitra, M.; Sengupta, S. *Induction Motor and Faults*; Springer: New York, NY, USA, 2016. [CrossRef]

73. Gawde, S.; Patil, S.; Kumar, S.; Kamat, P.; Kotecha, K.; Abraham, A. Multi-fault diagnosis of Industrial Rotating Machines using Data-driven approach: A review of two decades of research. *Eng. Appl. Artif. Intell.* **2023**, *123*, 106139. [CrossRef]

74. Cheng, C.; Ma, G.; Zhang, Y.; Sun, M.; Teng, F.; Ding, H.; Yuan, Y. A Deep Learning-Based Remaining Useful Life Prediction Approach for Bearings. *IEEE/ASME Trans. Mechatron.* **2020**, *25*, 1243–1254. [CrossRef]

75. Rezamand, M.; Kordestani, M.; Carriveau, R.; Ting, D.S.K.; Saif, M. An Integrated Feature-Based Failure Prognosis Method for Wind Turbine Bearings. *IEEE/ASME Trans. Mechatron.* **2020**, *25*, 1468–1478. [CrossRef]

76. Soualhi, A.; Medjaher, K.; Zerhouni, N. Bearing Health Monitoring Based on Hilbert–Huang Transform, Support Vector Machine, and Regression. *IEEE Trans. Instrum. Meas.* **2015**, *64*, 52–62. [CrossRef]

77. Gao, Z.; Cecati, C.; Ding, S.X. A survey of fault diagnosis and fault-tolerant techniques—Part I: Fault diagnosis with model-based and signal-based approaches. *IEEE Trans. Ind. Electron.* **2015**, *62*, 3757–3767. [CrossRef]

78. Lu, C.; Chen, J.; Hong, R.; Feng, Y.; Li, Y. Degradation trend estimation of slewing bearing based on LSSVM model. *Mech. Syst. Signal Process.* **2016**, *76*, 353–366. [CrossRef]

79. Shi, H.; Guo, J.; Bai, X.; Guo, L.; Liu, Z.; Sun, J. Gearbox Incipient Fault Detection Based on Deep Recursive Dynamic Principal Component Analysis. *IEEE Access* **2020**, *8*, 57646–57660. [CrossRef]

80. Zhao, M.; Tang, B.; Tan, Q. Bearing remaining useful life estimation based on time–frequency representation and supervised dimensionality reduction. *Measurement* **2016**, *86*, 41–55. [CrossRef]

81. Wang, Y.; Peng, Y.; Zi, Y.; Jin, X.; Tsui, K.L. A Two-Stage Data-Driven-Based Prognostic Approach for Bearing Degradation Problem. *IEEE Trans. Ind. Inform.* **2016**, *12*, 924–932. [CrossRef]

82. Jin, X.; Ma, E.; Cheng, L.; Pecht, M. Health Monitoring of Cooling Fans Based on Mahalanobis Distance With mRMR Feature Selection. *IEEE Trans. Instrum. Meas.* **2012**, *61*, 2222–2229. [CrossRef]

83. Si, Y.; Chen, Z.; Sun, J.; Zhang, D.; Qian, P. A Data-Driven Fault Detection Framework Using Mahalanobis Distance Based Dynamic Time Warping. *IEEE Access* **2020**, *8*, 108359–108370. [CrossRef]

84. Jin, X.; Wang, Y.; Chow, T.; Sun, Y. Mahalanobis Distance Based Approaches for System Health Monitoring: A Review. *IET Sci. Meas. Technol.* **2017**, *11*, 371–379. [CrossRef]

85. Shakya, P.; Kulkarni, M.; Darpe, A. Bearing diagnosis based on Mahalanobis-Taguchi-Gram-Schmidt method. *J. Sound Vib.* **2014**, *337*, 342–362. [CrossRef]

86. Wang, Z.; Lu, C.; Wang, Z.; Liu, H.; Fan, H. Fault diagnosis and health assessment for bearings using the Mahalanobis—Taguchi system based on EMD-SVD. *Trans. Inst. Meas. Control* **2013**, *35*, 798–807. [CrossRef]

87. Guo, L.; Li, N.; Jia, F.; Lei, Y.; Lin, J. A recurrent neural network based health indicator for remaining useful life prediction of bearings. *Neurocomputing* **2017**, *240*, 98–109. [CrossRef]

88. Zhou, H.; Huang, X.; Wen, G.; Lei, Z.; Dong, S.; Zhang, P.; Chen, X. Construction of health indicators for condition monitoring of rotating machinery: A review of the research. *Expert Syst. Appl.* **2022**, *203*, 117297. [CrossRef]

89. Jiang, G.; Xie, P.; He, H.; Yan, J. Wind Turbine Fault Detection Using a Denoising Autoencoder With Temporal Information. *IEEE/ASME Trans. Mechatron.* **2018**, *23*, 89–100. [CrossRef]

90. Chen, P.; Li, Y.; Wang, K.; Zuo, M.; Heyns, S.; Baggerohr, S. A threshold self-setting condition monitoring scheme for wind turbine generator bearings based on deep convolutional generative adversarial networks. *Measurement* **2020**, *167*, 108234. [CrossRef]

91. *ISO 20816-3:2022*; Mechanical Vibration—Measurement and Evaluation of Machine Vibration, Part 3: Industrial Machinery with a Power Rating Above 15 kW and Operating Speeds Between 120 r/min and 30,000 r/min. International Organization for Standardization: Geneva, Switzerland, 2022. Available online: https://www.iso.org/standard/78311.html (accessed on 29 October 2024).

92. *ISO 10816-8:2014*; Mechanical Vibration—Evaluation of Machine Vibration by Measurements on Non-Rotating Parts—Part 8: Reciprocating Compressor Systems. International Organization for Standardization: Geneva, Switzerland, 2014. Available online: https://www.iso.org/standard/18866.html (accessed on 29 October 2024).

93. Qin, Y.; Chen, D.; Xiang, S.; Zhu, C. Gated Dual Attention Unit Neural Networks for Remaining Useful Life Prediction of Rolling Bearings. *IEEE Trans. Ind. Inform.* **2021**, *17*, 6438–6447. [CrossRef]

94. Behzad, M.; Feizhoseini, S.; Arghand, H.A.; Davoodabadi, A.; Mba, D. Failure threshold determination of rolling element bearings using vibration fluctuation and failure modes. *Appl. Sci.* **2020**, *11*, 160. [CrossRef]

95. Wang, X.; Wang, T.; Ming, A.; Han, Q.; Chu, F.; Zhang, W.; Li, A. Deep spatiotemporal convolutional-neural-network-based remaining useful life estimation of bearings. *Chin. J. Mech. Eng.* **2021**, *34*, 62. [CrossRef]

96. Yang, S.; Tang, B.; Wang, W.; Yang, Q.; Hu, C. Physics-informed multi-state temporal frequency network for RUL prediction of rolling bearings. *Reliab. Eng. Syst. Saf.* **2024**, *242*, 109716. [CrossRef]

97. Ding, Y.; Jia, M.; Cao, Y. Remaining Useful Life Estimation Under Multiple Operating Conditions via Deep Subdomain Adaptation. *IEEE Trans. Instrum. Meas.* **2021**, *70*, 1–11. [CrossRef]

98. Jiang, F.; Ding, K.; He, G.; Lin, H.; Chen, Z.; Li, W. Dual-Attention-Based Multiscale Convolutional Neural Network With Stage Division for Remaining Useful Life Prediction of Rolling Bearings. *IEEE Trans. Instrum. Meas.* **2022**, *71*, 3525410. [CrossRef]

99. Meng, Z.; Li, J.; Yin, N.; Pan, Z. Remaining useful life prediction of rolling bearing using fractal theory. *Measurement* **2020**, *156*, 107572. [CrossRef]

100. Shi, Y.; Zhu, W.; Xiang, Y.; Feng, Q. Condition-based maintenance optimization for multi-component systems subject to a system reliability requirement. *Reliab. Eng. Syst. Saf.* **2020**, *202*, 107042. [CrossRef]

101. Diyin, T.; Jinrong, C.; Jinsong, Y. Remaining useful life prediction for engineering systems under dynamic operational conditions: A semi-Markov decision process-based approach. *Chin. J. Aeronaut.* **2019**, *32*, 627–638. [CrossRef]

102. Liu, D.; Zhou, J.; Liao, H.; Peng, Y.; Peng, X. A Health Indicator Extraction and Optimization Framework for Lithium-Ion Battery Degradation Modeling and Prognostics. *IEEE Trans. Syst. Man Cybern. Syst.* **2015**, *45*, 915–928. [CrossRef]

103. Tischmacher, H.; Tsoumas, I.P.; Gattermann, S. Probability model for discharge activities in bearings of converter-fed electric motors. In Proceedings of the 2014 International Conference on Electrical Machines (ICEM), Berlin, Germany, 2–5 September 2014; pp. 1818–1824. [CrossRef]

104. Ao, Y.; Laghrouche, S.; Depernet, D.; Chen, K. Proton Exchange Membrane Fuel Cell Prognosis Based on Frequency-Domain Kalman Filter. *IEEE Trans. Transp. Electrif.* **2021**, *7*, 2332–2343. [CrossRef]

105. Wang, X.; Al Imran, M.N.; Ali, M.; Zhang, B. Interdigital Capacitor Sensor-Based Cable Health Monitoring. *IEEE Trans. Ind. Electron.* **2023**, *70*, 7301–7309. [CrossRef]

106. Teng, W.; Han, C.; Hu, Y.; Cheng, X.; Song, L.; Liu, Y. A Robust Model-Based Approach for Bearing Remaining Useful Life Prognosis in Wind Turbines. *IEEE Access* **2020**, *8*, 47133–47143. [CrossRef]

107. Zhang, Z.X.; Si, X.S.; Hu, C.H. An Age- and State-Dependent Nonlinear Prognostic Model for Degrading Systems. *IEEE Trans. Reliab.* **2015**, *64*, 1214–1228. [CrossRef]

108. Li, N.; Lei, Y.; Yan, T.; Li, N.; Han, T. A Wiener-Process-Model-Based Method for Remaining Useful Life Prediction Considering Unit-to-Unit Variability. *IEEE Trans. Ind. Electron.* **2019**, *66*, 2092–2101. [CrossRef]

109. Zhai, Q.; Ye, Z.S. RUL Prediction of Deteriorating Products Using an Adaptive Wiener Process Model. *IEEE Trans. Ind. Inform.* **2017**, *13*, 2911–2921. [CrossRef]

110. Zhang, S.; Zhai, Q.; Shi, X.; Liu, X. A Wiener Process Model With Dynamic Covariate for Degradation Modeling and Remaining Useful Life Prediction. *IEEE Trans. Reliab.* **2023**, *72*, 214–223. [CrossRef]

111. Li, T.; Pei, H.; Pang, Z.; Si, X.; Zheng, J. A Sequential Bayesian Updated Wiener Process Model for Remaining Useful Life Prediction. *IEEE Access* **2020**, *8*, 5471–5480. [CrossRef]

112. Wang, C.; Yang, J.; Jie, H.; Tian, B.; Zhao, Z.; Chang, Y. An uncertainty perception metric network for machinery fault diagnosis under limited noisy source domain and scarce noisy unknown domain. *Adv. Eng. Inform.* **2024**, *62*, 102682. [CrossRef]

113. Jin, X.; Sun, Y.; Que, Z.; Wang, Y.; Chow, T.W.S. Anomaly Detection and Fault Prognosis for Bearings. *IEEE Trans. Instrum. Meas.* **2016**, *65*, 2046–2054. [CrossRef]

114. Cui, L.; Li, W.; Liu, D.; Wang, H. A novel robust dual unscented particle filter method for remaining useful life prediction of rolling bearings. *IEEE Trans. Instrum. Meas.* **2024**, *73*, 3509009. [CrossRef]

115. Li, G.; Wei, J.; He, J.; Yang, H.; Meng, F. Implicit Kalman filtering method for remaining useful life prediction of rolling bearing with adaptive detection of degradation stage transition point. *Reliab. Eng. Syst. Saf.* **2023**, *235*, 109269. [CrossRef]

116. Cui, J.; Cao, L.; Zhang, T. A two-stage Gaussian process regression model for remaining useful prediction of bearings. *Proc. Inst. Mech. Eng. Part O J. Risk Reliab.* **2024**, *238*, 333–348. [CrossRef]

117. Lu, Y.; Tang, D.; Zhu, D.; Gao, Q.; Zhao, D.; Lyu, J. Remaining useful life prediction for bearing based on coupled diffusion process and temporal attention. *IEEE Trans. Instrum. Meas.* **2024**, *73*, 3510310. [CrossRef]

118. Ye, Z.; Zhang, Q.; Shao, S.; Niu, T.; Zhao, Y. Rolling bearing health indicator extraction and RUL prediction based on multi-scale convolutional autoencoder. *Appl. Sci.* **2022**, *12*, 5747. [CrossRef]

119. Ren, L.; Sun, Y.; Cui, J.; Zhang, L. Bearing remaining useful life prediction based on deep autoencoder and deep neural networks. *J. Manuf. Syst.* **2018**, *48*, 71–77. [CrossRef]

120. de Pater, I.; Mitici, M. Developing health indicators and RUL prognostics for systems with few failure instances and varying operating conditions using a LSTM autoencoder. *Eng. Appl. Artif. Intell.* **2023**, *117*, 105582. [CrossRef]

121. Tao, L.; Yang, C.; Cheng, Y.; Lu, C.; Ragulskis, M. Machine component health prognostics with only truncated histories using geometrical metric approach. *Mech. Syst. Signal Process.* **2018**, *113*, 168–179. [CrossRef]

122. Yang, F.; Habibullah, M.S.; Zhang, T.; Xu, Z.; Lim, P.; Nadarajan, S. Health index-based prognostics for remaining useful life predictions in electrical machines. *IEEE Trans. Ind. Electron.* **2016**, *63*, 2633–2644. [CrossRef]

123. Hochreiter, S.; Schmidhuber, J. Long Short-Term Memory. *Neural Comput.* **1997**, *9*, 1735–1780. [CrossRef] [PubMed]

124. Xiang, S.; Qin, Y.; Zhu, C.; Wang, Y.; Chen, H. Long short-term memory neural network with weight amplification and its application into gear remaining useful life prediction. *Eng. Appl. Artif. Intell.* **2020**, *91*, 103587. [CrossRef]

125. Gupta, J.; Pathak, S.; Kumar, G. Deep learning (CNN) and transfer learning: A review. *J. Physics: Conf. Ser.* 2022, *2273*, 012029. [CrossRef]

126. Park, K.; Choi, Y.; Choi, W.J.; Ryu, H.Y.; Kim, H. LSTM-Based Battery Remaining Useful Life Prediction with Multi-Channel Charging Profiles. *IEEE Access* **2020**, *8*, 20786–20798. [CrossRef]

127. Shi, Z.; Chehade, A. A dual-LSTM framework combining change point detection and remaining useful life prediction. *Reliab. Eng. Syst. Saf.* **2021**, *205*, 107257. [CrossRef]

128. de Pater, I.; Mitici, M. Novel metrics to evaluate probabilistic remaining useful life prognostics with applications to turbofan engines. In Proceedings of the PHM Society European Conference, Turin, Italy, 6–8 July 2022; Volume 7, pp. 96–109. [CrossRef]

129. de Pater, I.; Reijns, A.; Mitici, M. Alarm-based predictive maintenance scheduling for aircraft engines with imperfect Remaining Useful Life prognostics. *Reliab. Eng. Syst. Saf.* **2022**, *221*, 108341. [CrossRef]

130. Li, X.; Ding, Q.; Sun, J.Q. Remaining useful life estimation in prognostics using deep convolution neural networks. *Reliab. Eng. Syst. Saf.* **2018**, *172*, 1–11. [CrossRef]

131. Berghout, T.; Benbouzid, M. A systematic guide for predicting remaining useful life with machine learning. *Electronics* **2022**, *11*, 1125. [CrossRef]

132. Chen, Z.; Li, W. Multisensor Feature Fusion for Bearing Fault Diagnosis Using Sparse Autoencoder and Deep Belief Network. *IEEE Trans. Instrum. Meas.* **2017**, *66*, 1693–1702. [CrossRef]

133. Zeng, L.; Zheng, J.; Yao, L.; Ge, Z. Dynamic Bayesian Networks for Feature Learning and Transfer Applications in Remaining Useful Life Estimation. *IEEE Trans. Instrum. Meas.* **2023**, *72*, 3500312. [CrossRef]

134. Hu, C.H.; Pei, H.; Si, X.S.; Du, D.B.; Pang, Z.N.; Wang, X. A Prognostic Model Based on DBN and Diffusion Process for Degrading Bearing. *IEEE Trans. Ind. Electron.* **2020**, *67*, 8767–8777. [CrossRef]

135. Al-Khazraji, H.; Nasser, A.R.; Hasan, A.M.; Al Mhdawi, A.K.; Al-Raweshidy, H.; Humaidi, A.J. Aircraft Engines Remaining Useful Life Prediction Based on A Hybrid Model of Autoencoder and Deep Belief Network. *IEEE Access* **2022**, *10*, 82156–82163. [CrossRef]

136. Zhang, C.; Lim, P.; Qin, A.K.; Tan, K.C. Multiobjective Deep Belief Networks Ensemble for Remaining Useful Life Estimation in Prognostics. *IEEE Trans. Neural Netw. Learn. Syst.* **2017**, *28*, 2306–2318. [CrossRef]

137. Vaswani, A.; Shazeer, N.; Parmar, N.; Uszkoreit, J.; Jones, L.; Gomez, A.N.; Kaiser, Ł.; Polosukhin, I. Attention is all you need. *Adv. Neural Inf. Process. Syst.* **2017**, *30*. [CrossRef]

138. Wang, C.; Tian, B.; Yang, J.; Jie, H.; Chang, Y.; Zhao, Z. Neural-transformer: A brain-inspired lightweight mechanical fault diagnosis method under noise. *Reliab. Eng. Syst. Saf.* **2024**, *251*, 110409. [CrossRef]

139. Chen, D.; Hong, W.; Zhou, X. Transformer Network for Remaining Useful Life Prediction of Lithium-Ion Batteries. *IEEE Access* **2022**, *10*, 19621–19628. [CrossRef]

140. Hu, Q.; Zhao, Y.; Ren, L. Novel Transformer-Based Fusion Models for Aero-Engine Remaining Useful Life Estimation. *IEEE Access* **2023**, *11*, 52668–52685. [CrossRef]

141. Goodfellow, I.; Pouget-Abadie, J.; Mirza, M.; Xu, B.; Warde-Farley, D.; Ozair, S.; Courville, A.; Bengio, Y. Generative adversarial nets. *Adv. Neural Inf. Process. Syst.* **2014**, *27*. [CrossRef]

142. Hakim, M.; Omran, A.A.B.; Ahmed, A.N.; Al-Waily, M.; Abdellatif, A. A systematic review of rolling bearing fault diagnoses based on deep learning and transfer learning: Taxonomy, overview, application, open challenges, weaknesses and recommendations. *Ain Shams Eng. J.* **2022**, *14*, 101945. [CrossRef]

143. Zhang, X.; Qin, Y.; Yuen, C.; Jayasinghe, L.; Liu, X. Time-Series Regeneration With Convolutional Recurrent Generative Adversarial Network for Remaining Useful Life Estimation. *IEEE Trans. Ind. Inform.* **2021**, *17*, 6820–6831. [CrossRef]

144. Ye, R.; Dai, Q. Implementing transfer learning across different datasets for time series forecasting. *Pattern Recognit.* **2021**, *109*, 107617. [CrossRef]

145. Gu, B.; Liu, Z. Transfer Learning-Based Remaining Useful Life Prediction Method for Lithium-Ion Batteries Considering Individual Differences. *Appl. Sci.* **2024**, *14*, 698. [CrossRef]

146. Severson, K.A.; Attia, P.M.; Jin, N.; Perkins, N.; Jiang, B.; Yang, Z.; Chen, M.H.; Aykol, M.; Herring, P.K.; Fraggedakis, D.; et al. Data-driven prediction of battery cycle life before capacity degradation. *Nat. Energy* **2019**, *4*, 383–391. [CrossRef]

147. Fan, Y.; Nowaczyk, S.; Rögnvaldsson, T. Transfer learning for remaining useful life prediction based on consensus self-organizing models. *Reliab. Eng. Syst. Saf.* **2020**, *203*, 107098. [CrossRef]

148. Huang, J.; Yuan, M.; Cui, J.; Zhao, J.; Qu, Y.; Dong, S. LSTM and ELM based transfer learning approach for online bearing remaining useful life prediction. In Proceedings of the 12th International Conference on Quality, Reliability, Risk, Maintenance, and Safety Engineering (QR2MSE 2022), Emeishan, China, 27–30 July 2022; IET: Edison, NJ, USA, 2022; Volume 2022, pp. 1448–1455. [CrossRef]

149. Chen, J.; Huang, R.; Chen, Z.; Mao, W.; Li, W. Transfer learning algorithms for bearing remaining useful life prediction: A comprehensive review from an industrial application perspective. *Mech. Syst. Signal Process.* **2023**, *193*, 110239. [CrossRef]

150. Wei, Y.; Wu, D. State of health and remaining useful life prediction of lithium-ion batteries with conditional graph convolutional network. *Expert Syst. Appl.* **2024**, *238*, 122041. [CrossRef]

151. Wang, Y.X.; Zhao, S.; Wang, S.; Ou, K.; Zhang, J. Enhanced vision-transformer integrating with semi-supervised transfer learning for state of health and remaining useful life estimation of lithium-ion batteries. *Energy AI* **2024**, *17*, 100405. [CrossRef]

152. Kim, G.; Choi, J.G.; Lim, S. Using transformer and a reweighting technique to develop a remaining useful life estimation method for turbofan engines. *Eng. Appl. Artif. Intell.* **2024**, *133*, 108475. [CrossRef]

153. Zhu, D.; Lyu, J.; Gao, Q.; Lu, Y.; Zhao, D. Remaining useful life estimation of bearing using spatio-temporal convolutional transformer. *Meas. Sci. Technol.* **2024**, *35*, 045126. [CrossRef]

154. Zheng, G.; Li, Y.; Zhou, Z.; Yan, R. A Remaining Useful Life Prediction Method of Rolling Bearings Based on Deep Reinforcement Learning. *IEEE Internet Things J.* **2024**. [CrossRef]

155. Li, J.; Li, S.; Fan, Y.; Ding, Z.; Yang, L. Remaining useful life prediction of bearings using a trend memory attention-based GRU network. *Meas. Sci. Technol.* **2024**, *35*, 055001. [CrossRef]

156. Li, H.; Zhang, Z.; Li, T.; Si, X. A review on physics-informed data-driven remaining useful life prediction: Challenges and opportunities. *Mech. Syst. Signal Process.* **2024**, *209*, 111120. [CrossRef]

157. Zang, Y.; Shangguan, W.; Cai, B.; Wang, H.; Pecht, M.G. Hybrid remaining useful life prediction method. A case study on railway D-cables. *Reliab. Eng. Syst. Saf.* **2021**, *213*, 107746. [CrossRef]

158. Chang, Y.; Fang, H.; Zhang, Y. A new hybrid method for the prediction of the remaining useful life of a lithium-ion battery. *Appl. Energy* **2017**, *206*, 1564–1578. [CrossRef]

159. Yan, M.; Wang, X.; Wang, B.; Chang, M.; Muhammad, I. Bearing remaining useful life prediction using support vector machine and hybrid degradation tracking model. *ISA Trans.* **2020**, *98*, 471–482. [CrossRef] [PubMed]

160. Wang, F.K.; Mamo, T. Hybrid approach for remaining useful life prediction of ball bearings. *Qual. Reliab. Eng. Int.* **2019**, *35*, 2494–2505. [CrossRef]

161. Raissi, M.; Perdikaris, P.; Karniadakis, G.E. Physics-informed neural networks: A deep learning framework for solving forward and inverse problems involving nonlinear partial differential equations. *J. Comput. Phys.* **2019**, *378*, 686–707. [CrossRef]

162. Deng, Y.; Du, S.; Wang, D.; Shao, Y.; Huang, D. A calibration-based hybrid transfer learning framework for RUL prediction of rolling bearing across different machines. *IEEE Trans. Instrum. Meas.* **2023**, *72*, 3511015. [CrossRef]

163. Yucesan, Y.A.; Viana, F.A. A hybrid physics-informed neural network for main bearing fatigue prognosis under grease quality variation. *Mech. Syst. Signal Process.* **2022**, *171*, 108875. [CrossRef]

164. Liao, L.; Köttig, F. Review of hybrid prognostics approaches for remaining useful life prediction of engineered systems, and an application to battery life prediction. *IEEE Trans. Reliab.* **2014**, *63*, 191–207. [CrossRef]

165. Nascimento, R.G.; Corbetta, M.; Kulkarni, C.S.; Viana, F.A. Hybrid physics-informed neural networks for lithium-ion battery modeling and prognosis. *J. Power Sources* **2021**, *513*, 230526. [CrossRef]

166. Fernández, J.; Corbetta, M.; Kulkarni, C.S.; Chiachío, J.; Chiachío, M. Training of physics-informed Bayesian neural networks with ABC-SS for prognostic of Li-ion batteries. *Comput. Ind.* **2024**, *155*, 104058. [CrossRef]

167. Chen, X.; Ma, M.; Zhao, Z.; Zhai, Z.; Mao, Z. Physics-informed deep neural network for bearing prognosis with multisensory signals. *J. Dyn. Monit. Diagn.* **2022**, *1*, 200–207. [CrossRef]

168. Ogunsanya, M.; Isichei, J.; Desai, S. Grid search hyperparameter tuning in additive manufacturing processes. *Manuf. Lett.* **2023**, *35*, 1031–1042. [CrossRef]

169. Injadat, M.; Moubayed, A.; Nassif, A.B.; Shami, A. Systematic ensemble model selection approach for educational data mining. *Knowl.-Based Syst.* **2020**, *200*, 105992. [CrossRef]
170. Bergstra, J.; Bengio, Y. Random search for hyper-parameter optimization. *J. Mach. Learn. Res.* **2012**, *13*, 281–305.
171. Snoek, J.; Larochelle, H.; Adams, R.P. Practical bayesian optimization of machine learning algorithms. *Adv. Neural Inf. Process. Syst.* **2012**, *25*. [CrossRef]
172. Li, L.; Jamieson, K.; DeSalvo, G.; Rostamizadeh, A.; Talwalkar, A. Hyperband: A novel bandit-based approach to hyperparameter optimization. *J. Mach. Learn. Res.* **2018**, *18*, 1–52.
173. Bengio, Y. Gradient-based optimization of hyperparameters. *Neural Comput.* **2000**, *12*, 1889–1900. [CrossRef]
174. Lessmann, S.; Stahlbock, R.; Crone, S.F. Optimizing Hyperparameters of Support Vector Machines by Genetic Algorithms. In Proceedings of the IC-AI, Las Vegas, NV, USA, 27–30 June 2005; Volume 74, p. 82.
175. Ma, H.; Zhang, Y.; Sun, S.; Liu, T.; Shan, Y. A comprehensive survey on NSGA-II for multi-objective optimization and applications. *Artif. Intell. Rev.* **2023**, *56*, 15217–15270. [CrossRef]
176. Saxena, A.; Celaya, J.; Balaban, E.; Goebel, K.; Saha, B.; Saha, S.; Schwabacher, M. Metrics for evaluating performance of prognostic techniques. In Proceedings of the 2008 International Conference on Prognostics and Health Management, Denver, CO, USA, 6–9 October 2008; pp. 1–17. [CrossRef]
177. Saxena, A.; Celaya, J.; Saha, B.; Saha, S.; Goebel, K. On applying the prognostic performance metrics. In Proceedings of the Annual Conference of the PHM Society, San Diego, CA, USA, 27 September–1 October 2009; Volume 1.